5-2015

A Phylogenetic Analysis of Dictyostelium purpureum Based on Nuclear rDNA Sequences

Mahmoud Suliman
University of Arkansas, Fayetteville

A Phylogenetic Analysis of *Dictyostelium purpureum* Based on Nuclear rDNA Sequences

A Phylogenetic Analysis of *Dictyostelium purpureum* Based on Nuclear rDNA Sequences

A thesis submitted in partial fulfillment
of the requirements for the degree of
Master of Science in Cell and Molecular Biology

by

Mahmoud Suliman
Technion - Israel Institute of Technology
Bachelor of Science in Biotechnology and Food Engineering, 2010

May 2015
University of Arkansas

This thesis is approved for recommendation to the Graduate Council.

_____
Dr. Steven L. Stephenson
Thesis Director

_____ _____
Dr. Fred Spiegel
Committee Member

Dr. Jeffrey A. Lewis
Committee Member

_____
Dr. Allen Lawrence Szalanski
Committee Member

Abstract

Dictyostelids (cellular slime molds) are eukaryotic microorganisms that have both unicellular and multicellular stages during their life cycle. In this study, a molecular phylogenetic analysis was conducted for isolates of one species (*Dictyostelium purpureum*) based DNA sequences of the ITS, 5.8S and SSU regions of nuclear rDNA. Moreover, a detailed morphological study was carried out using images obtained with both dissecting and compound microscopes. Mating experiments were carried out to assess macrocysts formation between each pair of isolates. The constructed molecular phylogenetic trees indicate that (1) *D. purpureum* isolates are more closely related to each other than to other species of dictyostelids and (2) several subgroups can be noted within the total isolates of *D. purpureum.*

Acknowledgments

I would like to especially thank my thesis director, Dr. Steven Stephenson, for his unwavering support during this research. I would like to acknowledge the advice and guidance from my thesis committee, Dr. Frederick Speigel, Dr. Jeffrey Lewis, and Dr. Allen Szalanski. I would like to express my gratitude to the United States International Fulbright Exchange Program for my sponsorship at the University of Arkansas. I would like to recognize the contributions of Dr. John Landolt and Dr. James Cavender for kindly providing me with isolates of *D. purpureum*. I wish to express my sincere thanks to Dr. Amber Tribodi, Alex Tice, Fareed Mahammed, and Clint Trammel for their support and assistance during my research. Thanks to all my fellow lab-mates and colleagues for their support and cooperation throughout my study at the University of Arkansas.

Table of Contents

Introduction

Dictyostelids (cellular slime molds) are eukaryotic microorganisms that have both unicellular and multicellular stages during their life cycle (Raper 1984). For this reason, dictyostelids are widely used in biological research, including the study of cell differentiation, genetics and cell signaling pathways (Schaap 2011). One model organism and a widely investigated species is *Dictyostelium discoideum* Raper, as its complete genomic sequence is known and this organism is simple to culture and investigate (Annesley and Fisher 2009). The age of dictyostelids is estimated to be more than 400 million years (Sucgang et al. 2011), and they were first discovered by Oscar Brefeld in 1869, with the isolation of the widespread species *Dictyostelium mucoroides* Bref. (Brefeld 1869, Raper 1984). The introduction of a new isolation method for dictyostelids (Cavender and Raper 1965) enabled the discovery of new species from many different areas around the world (Cavender 2013).

Ecology and Distribution

There are approximately 150 described species of dictyostelids, and more species are expected to be discovered in the future (Romeralo et al. 2012). Dictyostelids occur in almost any type of soil, and are affected by environmental conditions such as temperature, pH, moisture, and plant cover (Raper 1984). Moreover, the diversity and occurrence of dicyostelids increase with a decrease in latitude and elevation. However, different species of dictyostelids do not have the same preferences for particular environmental conditions. Dictyostelids feed on bacteria in the soil, which can influence the bacteria abundance and diversity in the soil, and therefore the soil properties (Swanson et al. 1999).

Spore dispersal is the main way for reproduction and distribution of dictyostelids. Spores can be carried by water currents, birds, soil vertebrates, and other soil organisms (Stephenson and Landolt 1992, Swanson et al. 1999, Cavender 2013). Spore dispersal is less likely to be airborne, due to the presence of a slimy sheath that surrounds the spores (Cavender 2013).

Dictyostelids Taxonomy

Dictyostelids are a monophyletic group under the supergroup Amoebozoa, as shown in Figure 1 (Adl et al. 2012). Traditionally, dictyostelids have been classified into three genera according to morphological characteristics. These are *Dictyostelium*, *Polysphondylium*, and *Actyostelium* (Raper 1984). *Dictyostelium* is considered as the largest group within the dictyostelids and includes the most common species, *D. mucoroides*, found in almost any type of soil. This group is characterized by a cellular sorophore and non-branched sorocarps or branching without any organized pattern. *Polysphondylium* was discovered by Brefeld in 1884 and is also characterized by a cellular sorophore, while the main difference is the presence of branches in whorls. *Actyostelium* is the last discovered group and is very rare in nature. It is characterized by its small size, lack of color, and acellular sorophores (Raper 1984).

However, the first molecular studies reclassified dictyostelids into four major groups (Schaap et al. 2006). Further studies added additional smaller groups to this classification, referred as the *Polycarpum*, *Violaceum* and *Polycephalum* Complexes (Romeralo et al. 2011). This classification was modified using genomic data, while placing the root of dictyostelids between the branches of groups 1-2 and 3-4. In this classification, group 1 includes only species of *Dictyostelium*. Group 2A includes all the species of *Actyostelium* with the exception of *Actyostelium ellipticum* Cavender, while group 2B combines species from all of the three

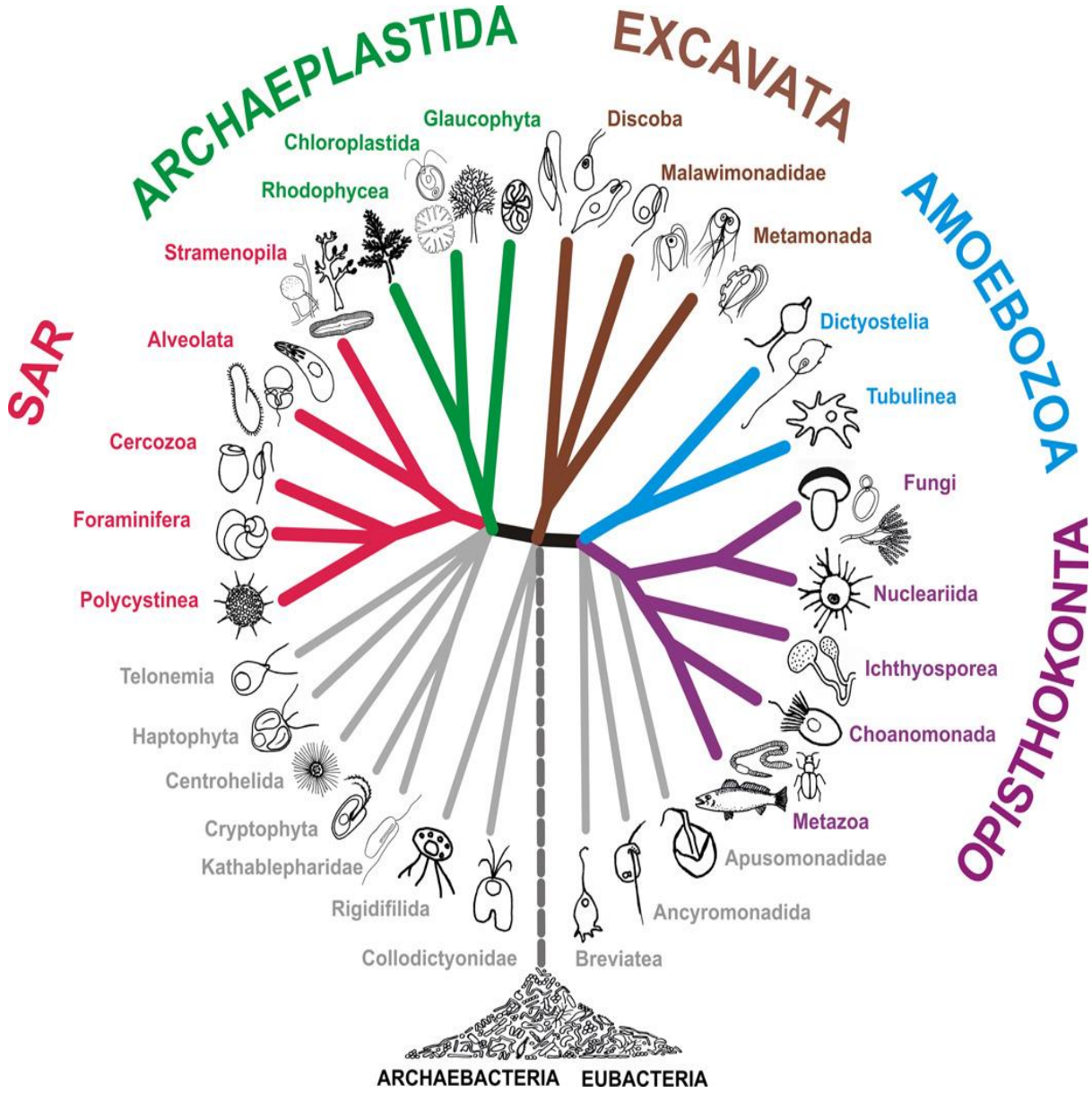

Figure 1. Eukaryote phylogeny after Adl et al. (2012). This classification divides the eukaryotes into the five supergroups Sar, Archaeplastida, Excavata, Amoebozoa, and Opisthokonta, and few smaller groups. Dictyostelids are classified under the supergroup Amoebozoa.

traditional groups. Groups 3 and 4 include only species of *Dictyostelium* (Romeralo and Fiz-Palacios 2013).

Molecular markers used for the study of dictyostelids include the small subunit ribosomal DNA (SSU rDNA) and 5.8S rDNA with the flanking internal transcribed spacers (ITS1 and ITS2) (Schaap et al. 2006, Romeralo et al. 2007, Romeralo et al. 2010). Several studies have focused on one species of dictyostelids using rDNA markers, such as *Dictyostelium purpureum* Olive (Mehdiabadi et al 2009), *Dictyostelium sphaerocephalum* (Oudem) Sacc and Marchal (Romeralo et al. 2007), and *Dictyostelium rosarium* Raper and Cavender (Romeralo et al. 2010). Moreover, new species identifications, such as D*ictyostelium ibericum,* were carried out using ITS and SSU rDNA markers (Romeralo et al. 2009). Other molecular markers used for the study of dictyostelids included the mitochondrial marker ATPase1 (Perrigo 2013), α-tubulin (Schaap et al. 2006), and Inter Simple Sequence Repeats-PCR (ISSR-PCR) (Januszewska 2011).

Life Cycle

Dictyostelids have sexual and asexual life cycles that include both unicellular and multicellular stages (Raper 1984). Environmental conditions such as light, temperature, moisture, and the growth medium can affect the preference of the life cycle (Nickerson and Raper 1973). Nutrient availability favors the sexual life cycle (Suzuki and Yanagisawa 1989), while starvation encourages the asexual life cycle (Blaskovics and Raper 1957). The sexual life cycle is more likely to happen in dark conditions, with high levels of moisture and temperature (20-25 ^{0}C) that can assist in the formation of macrocysts (Nickerson and Raper 1973). Another important factor is the presence of calcium necessary for the process of cell fusion (Chagla and Lewis 1980).

Several species of dictyostelids have an encystation stage in the life cycle, termed a microcyst (Raper 1984). Microcyst formation includes only one cell and involves the formation

of a cell wall and entering a dormancy stage, which is considered a survival mechanism in drought conditions (Budniak and O'Day 2012). Higher osmotic pressure stimulates the formation of the encystment stages in the social amoebae, whereas lower osmotic levels induce the germination of the microcysts to form free living amoebae (Toama and Raper, 1967). The alternative life cycles of dictyostelids are demonstrated in Figure 2.

Asexual Life Cycle

The asexual life cycle consists of several stages that include a vegetative stage, cell aggregation, and fructification, as shown in Figure 3 (Raper 1984, Hagiwara 1989, Myre 2012). The life cycle begins with the germination of the amoebae from the spores. One feature of the spores is the existence of auto inhibitors to allow germination only when spores are at low density (Raper 1984). This germination starts with the activation of the spores as a response to environmental changes, followed by swelling, forming of contractile vacuole, and finally the breakup of the spore wall and the emergence of a free living amoeba (Cotter and Raper 1966). The amoebae feed on bacteria and divide by binary fission (Hagiwara 2007). The cell aggregation stage is the switch from the unicellular to the multicellular living stage, named a pseudoplasmodium. The flow of the amoebae toward the aggregation centers starts as a response to a chemotactic substance secreted by the cells (Raper 1984, Hagiwara 1989). Sorogens emerge from the aggregation centers at the beginning of the fructification stage and may or may not migrate before giving rise to fruiting bodies, named sorocarps (Hagiwara 1989). The sorocarps consist of stalk cells and spores (Schaap et al. 2006). All of the stages from spore germination until the formation of fruiting bodies are haploid stages (Hagiwara 1989).

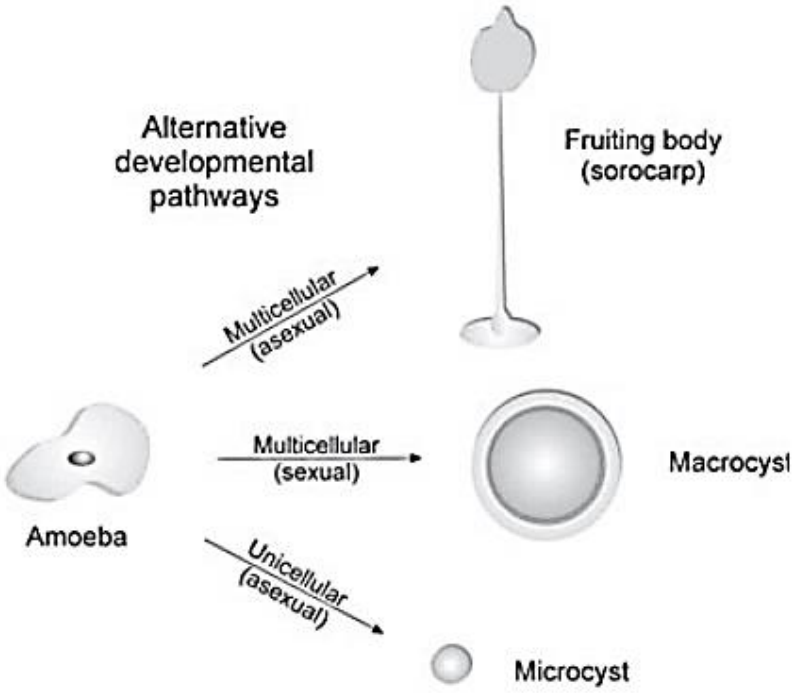

Figure 2. Alternative development pathways in the dictyostelids (from O'Day and Keszei ([2012]). © Reproduced with permission of the publisher, John Wiley and Sons, 2015.

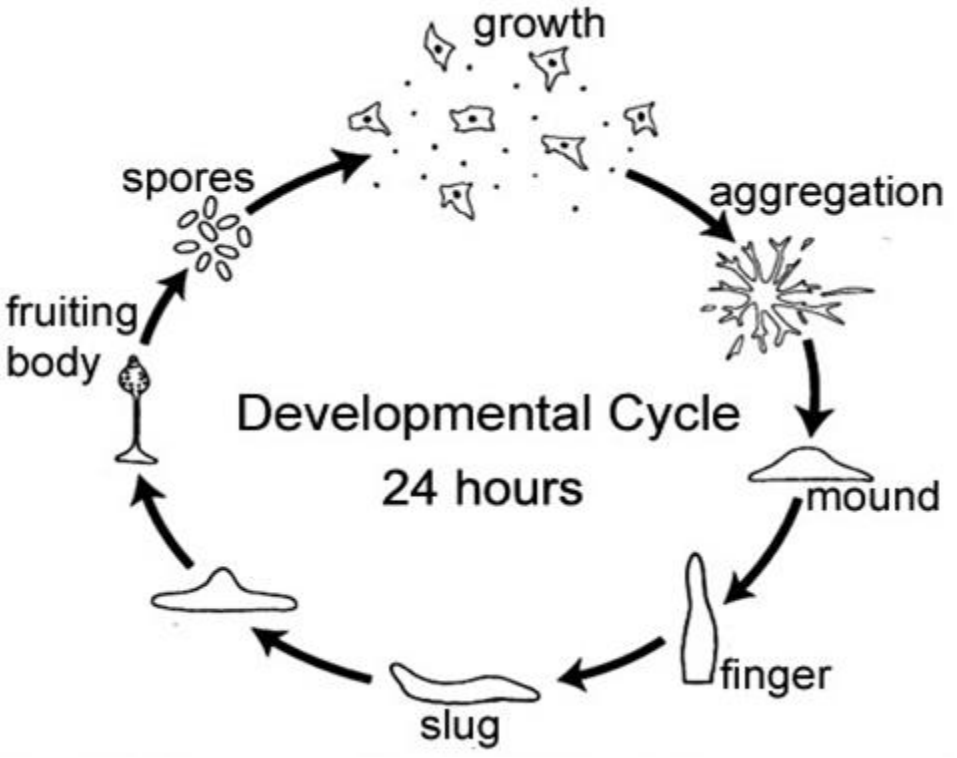

Figure 3. Diagram of the life cycle of *D. discoideum*, from spore dispersal, vegetative growth of free living amebae, aggregation, slug migration, and fruiting body formation, adapted and modified from Myre (2012).

Sexual Life Cycle

The sexual life cycle involves the fusion of two haploid cells that belong to two different mating types to form a diploid zygote (Bloomfield 2013). The zygote attracts other haploid cells by secreting special chemoattractants (Abe et al. 1984), followed by phagocytosis of the cells (Blaskovics and Raper 1957, Filosa and Dengler 1972). The next stage involves producing a cellulose-containing wall to form a macrocyst (Blaskovics and Raper 1957), and can last several weeks (Raper 1984). Nutrients from the cells are consumed by the macrocyt, using enzymes secreted from the lysosome (Erdos et al. 1973). The last stages of the sexual life cycle are meiosis and mitosis to form haploid cells (Erdos et al. 1973). Macrocyst production can be homothallic, produced by the same strains, or heterothallic between different strains (Bloomfield 2013). A diagram showing the macrocyst development in the sexual life cycle of *D. discoideum* is provided in Figure 4.

Dictyostelids Morphology

In general, dictyostelids have a low diversity of morphological characteristics, which indicates a small effect of natural selection on their evolution (Bonner 2013). As noted earlier, dictyostelid growth can be influenced by environmental conditions such as light, temperature, moisture, and the type of growth medium. The morphological description includes spores, aggregation patterns, fruiting body formation, and growth habit characteristics. The fruiting body of a dictyostelids, as shown in Figure 5, consists of a base, stalk, and a tip surrounded by a mass of spores called a sorus (Raper 1984). The growth habit can be solitary, gregarious, clustered, or a coremium-like structure. The branching in sorocarps can be regular with whorls, monochasium-like, or it can be irregular with sparse or crowded branches (Hagiwara 1989).

There are four types of aggregation patterns. The *mucoroides* type is aggregation toward

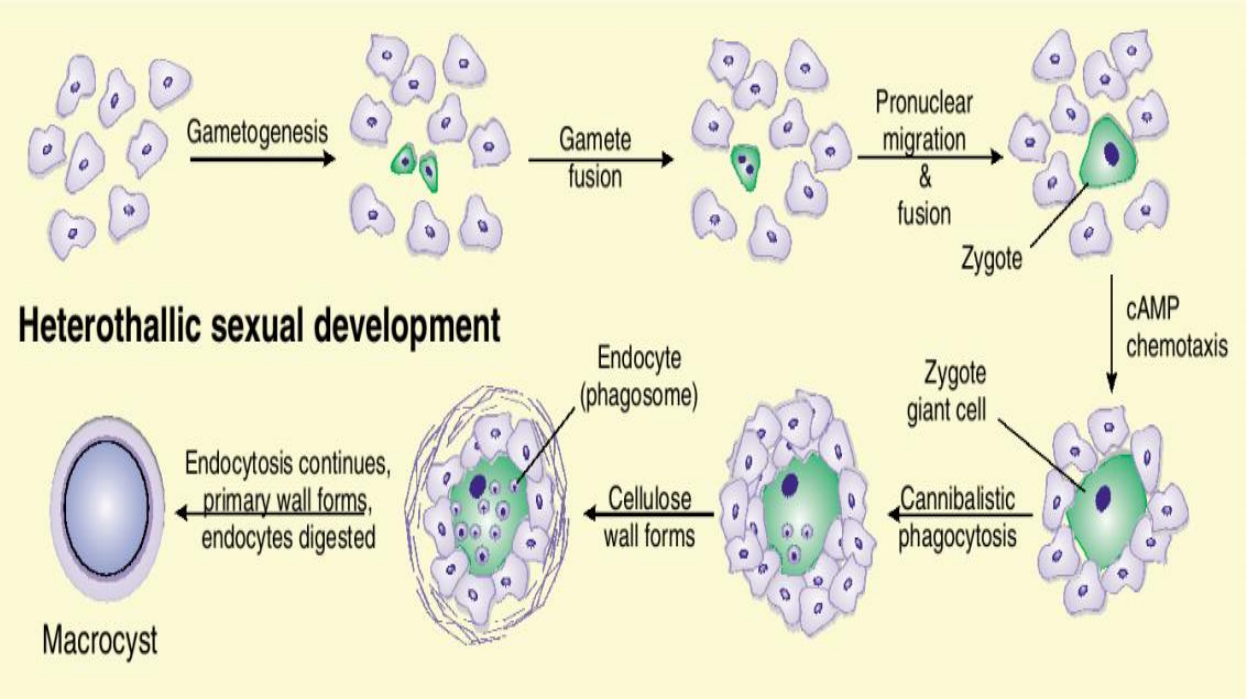

Figure 4. Sexual life cycle of *Dictyostelium discoideum*, from O'Day and Keszei (2012).

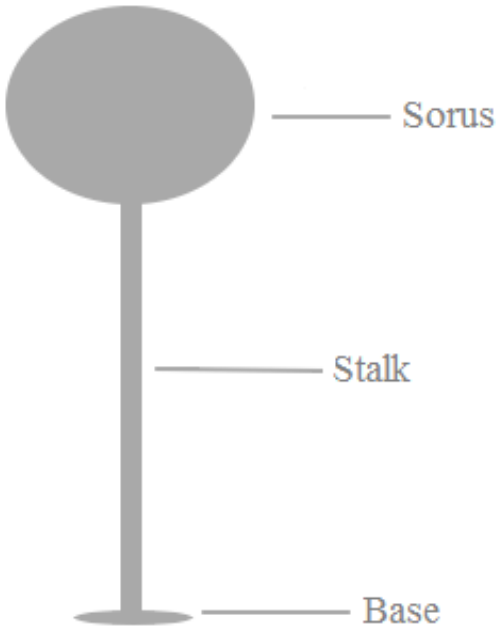

Figure 5. Fruiting body structure of dictyostelids, consisting of a base, stalk, and sorus.

the center in streams, with one or more sorocarps forming in the center. The *violaceum* type aggregation is radial, with several sorocarps emerging from aggregation centers along the radial streams around the main aggregation. The *minutum* type aggregation lacks the formation of streams, and one or more sorocarps are formed in the center. The *microsporum* type aggregation is also without the formation of streams, but with several sorocarps gradually forming from aggregation centers around the main aggregation (Hagiwara 1989).

Spores can have or lack granules and can be oblong, elliptical, fusiform, spherical, reniform, or sigmoid. However, some spores can be different and exceptionally larger than the regular spores (Hagiwara 1989). The presence and the absence of the polar granules, as well as their position in the spores are used as an important classification characteristics (Raper 1984).

Tips and bases morphology are also important characteristics for the study of dictyostelids (Hagiwara 1989). The bases can have supporters, or basal disc structures (Schaap 2007). The sorus, a mass of spores surrounded by a slime matrix, can be supported by an upper and a lower cap (Schaap 2007). The sorus is usually white but it can also have different colors (Hagiwara 1989).

Dictyostelium purpureum

Dictyostelium purpureum was first isolated by E. W. Olive in August 1897 from a mouse dung culture in Indiana. It is characterized by a purple colored sorus that turns black when mature, and oval spores with the dimensions 3-5 X 5-8 µm (Olive 1901). *Dictyostelium purpureum* can be found on the dung of animals, in soil, and on decayed leaf cover (Raper 1984), and occurs most often in limestone forests (Cavender 2013). Hagiwara (1992) reported two forms of *D. purpureum*. These are a temperate form with large sorocarps and elongated spores and a suptropical form with black sori and thick spores. Macrocysts and the sexual life cycle

have been observed in several strains of *D. purpureum* (Raper 1984). However, microcysts have not been observed (Raper 1984). The acrasin of *D. purpureum* is cAMP (Raper 1984). A detailed morphological description of the species *D. purpureum* as described by Raper (1984) and Hagiwara (1989) is provided in Table 1.

Dictyostelium purpureum is classified in group 4 within the dictyostelids, based on SSU and ITS rDNA markers (Schaap et al. 2006, Romeralo et al. 2010, Romeralo et al. 2011). Mehdiabadi et al. (2009) carried out a phylogenetic study of isolates of *D. purpureum* that originated from the United States and Japan. This study revealed the presence of three distinct groups of dictyostelids, as shown in Figure 6. Moreover, mating experiments for the same isolates showed that macrocyst formation is more likely to happen between isolates of the same group rather than between different groups (Mehdiabadi et al. 2009).

Objective

The purpose of the study described herein was to use DNA sequences of the ITS, 5.8S and SSU regions of nuclear rDNA to resolve the phylogeny of isolates of *D. purpureum* relative to other species of dictyostelids and within the same species while working with isolates from geographically distant localities. The choice of the nuclear rDNA gene for the molecular phylogenetic study is due to the presence of both conserved and variable regions. Moreover, this study tests the previous hypothesis from Mehdiabadi et al (2009) about the presence of three distinct groups A, B, and C within *D. purpureum* isolates. To better understand the phylogenetic relationships among the studied isolates, morphological studies and mating experiments were also conducted.

Table 1. Published morphological descriptions of *Dictyostelium purpureum*.

Morphological Characteristic	Hagiwara (1989)	Raper (1984)
Spore shape	Elliptical	Elliptical or capsule
Spores granules	Without polar granules, sometimes with irregular granules	Sometimes showing evidence of limited polar granules.
Spores diameter	6.7-7.2 X 2.4-3.1 µm	Often 5.0-7.2 X 2.5-3.2 µm
Mode of aggregation	Radial	Streaming
Slug migration	After sorophore formation	Not mentioned
Aggregation size	0.4-5 mm	One cm in diameter or more
Sorocarp habit	Solitary	Usually solitary
Branching pattern	Unbranched	Not mentioned
Stalk length	5.75 ± 2.09 mm	Can reach several centimeters
Stalk diameter	Tapering from base to tip	Generally 20-40 um in the base and tapering to half at the tip
Sorus diameter	40-300 µm	Mostly 125-450 µm

Table 1. (Cont.)

Morphological characteristic	Hagiwara (1989)	Raper (1984)
Sori color and shape	Pale to dark purple, globose	Dark vinaceous purple to almost black when mature, globose to citriform
Cellular support	Often with basal discs, with supporters if prostrate	Robust, with bases not enlarged
Cell diameter	Not mentioned	12-18 X 10-15 μm
Stalk shape	Erect or inclined	At first erect or semi-erect, then inclined
Stalk tip shape	Capitate	Not mentioned
Phototropism	Strongly phototropic	Strongly phototropic

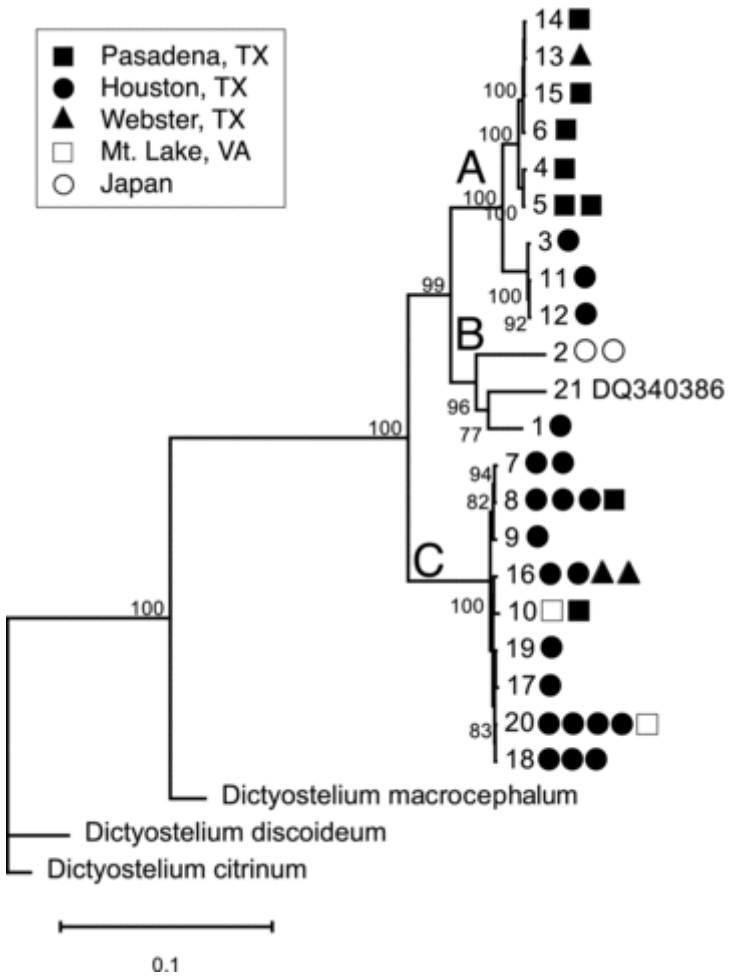

Figure 6. Bayesian phylogenetic analysis of *Dictyostelium purpureum*. Three groups, labeled with the letters A, B, and C, can be observed from the molecular phylogenetic tree (from Mehdiabadi et al. [2009]). © Reproduced with permission of the publisher, John Wiley and Sons, 2015.

Materials and Methods

Dictyostelium purpureum isolates culturing and maintaining

Eleven isolates that were morphologically identified as the species *D. purpureum* based on previous descriptions (Olive 1901, Raper 1984, Hagiwara 1989), and isolated from geographically distinct locations were obtained, as provided in Table 2. The isolates were obtained as spores preserved on silica gel, lyophilized in glass tubes, or suspended in a drop of dry milk on a piece of paper. The isolates were maintained on low nutrient agar plates, with *E. coli* as a food source, and subcultured regularly for morphological and molecular studies. Agar plates were prepared by dissolving 15 grams of agar in 1 liter of distilled water, and autoclaving it for 15 minutes at 400 °C.

For long-term storage, the isolates were preserved using silica gel, by generally following the protocol described by Raper (1984). Five milliliter glass tubes were filled with silica gel beads up to 1-2 cm, plugged with cotton, and sterilized in the oven for 90 minutes at 180 °C. The glass tubes were stored at 4 °C until needed. Spores from several fruiting bodies on the cultured plates were suspended in 0.5 ml of a sterile solution of nonfat dry milk. The suspension was added to the silica gel tubes that were precooled for 30 minutes on ice to prevent damage from the heat that may be released from the silica gel. The tubes were mixed thoroughly and put back on the ice for another 10 minutes and stored with cotton plugs at 4 °C. Resuspension of the spores after storage was performed by adding several silica gel granules together with *E. coli* suspension on the surface of the agar plates.

The identification of the isolates as the species of *D. purpureum* was performed based on the morphological description from the literature, and mainly by the dark color of the sori (Raper 1984, Hagiwara 1989).

Table 2. Isolates of *Dictyostelium purpureum*, their source, locality, and year of collection.

Species	Isolate	Source	Location	Date
D. purpureum	M8B	John Landolt	Madagascar	2009
D. purpureum	1A1Ba 2490	John Landolt	Cuba	2002
D. purpureum	MK11B 2522	John Landolt	Kenya	2005
D. purpureum	TL5B1 2857	John Landolt	Thailand	2009
D. purpureum	NB1B 2271	John Landolt	Queensland, Australia	2003
D. purpureum	GC4ADP 815	John Landolt	USA, Great Smoky Mountains National Park	2004
D. purpureum	GC1B 807	John Landolt		
D. purpureum	EQ4C 321	John Landolt	Ecuador	1998
D. purpureum	TRII-1 OH278	James Cavender	Costa Rica, Guanacaste Province	1961
D. purpureum	Za2a OH216	James Cavender	Costa Rica, Alajuela Province	1961
D. purpureum	F0II-4 OH283	James Cavender	Costa Rica, Limon Province	1961

Molecular Work

DNA Extraction, PCR Amplification and Sequencing

DNA extraction from several fruiting bodies of each isolate of *D. purpureum* was carried out following a salting-out method while using reagents prepared in the laboratory (Sambrook et al. 2001). PCR was conducted with the following primers. Approximately 1000 base pairs of the nuclear rDNA internal transcribed region that includes ITS1, ITS2, and the 5.8S genes were amplified using the primers 5'-GAGGAAGGAGAAGTCGTAACAAGGTATC-3' and 5-'GCTTACTGATATGCTTAAGTTCAGCGGG-3' (Romeralo et al. 2007). DNA amplification for around 2000 base pairs of the SSU rDNA was performed using the primers 18S-FA 5'-AACCTGGTTGATCCTGCCAG-3' and 18S-RB 5'-TGATCCTTCTGCAGGTTCAC-3' (Medlin et al. 1988, Perrigo 2013). DNA sequencing was done with the same primers, together with the two internal primers D542F 5'-ACAATTGGAGGGCAAGTCTG-3' and D1340R 5'-TCGAGGTCTCGTCCGTTATC -3' (Schaap et al. 2006). The polymerase chain reaction (PCR) for the amplification of the ITS rDNA region was carried out using a thermal cycler (C1000 Touch Thermal Cycler, Bio-Rad, Hercules, CA), starting with an initial denaturation at 95 °C for 5 min followed by 30 cycles of 94 °C for 1 min, 50 °C for 1 min, and 72 °C for 2 min, and a final extension at 72 °C for 10 min (Romeralo et al. 2010). The polymerase chain reaction (PCR) for the amplification of the SSU rDNA region was carried out using a thermal cycler (C1000 Touch Thermal Cycler, Bio-Rad, Hercules, CA), starting with an initial denaturation at 95 °C for 5 min followed by 30 cycles of 95 °C for 30 sec, 56 °C for 1 min, and 72 °C for 2 min, and a final extension at 72 °C for 10 min (Perrigo et al. 2013). PCR reactions included, 2-5 µl of extracted DNA, 1 µl of each primer (20 µm), 5 µl of 10X PCR buffer (New England BioLabs, Ipswich,

Massachusetts), 1 µl from each of the four nucleotides (20 µM), 0.4 µl of *Taq* polymerase (New England BioLabs, Ipswich, MA), and distilled water to a total volume of 50 µl.

A five µl portion of the amplified DNA from each sample was run at 165 V on a 2% agarose gel, that was stained with ethidium bromide, and visualized under UV light (BioDocit Imaging System, UVP, LLC, Upland, California). A 100 base pairs DNA ladder was run on a separate lane to estimate the size of the amplified fragments. The PCR products were purified using NANOSEP 30K OMEGA and NANOSEP 100K OMEGA (Pall Corporation, Port Washington, New York). One µl of the purified DNA was run on a 1% agarose gel for a purification check. Samples were sent to Eurofins MWG Operon (Huntsville, Alabama) for DNA sequencing in both directions.

Molecular Data Analysis

DNA sequences were edited manually using sequencer version 5.1 (Gene Codes Corporation, Ann Arbor, Michigan). Multiple sequence alignments were performed with other dictyostelid ITS and SSU rDNA sequences downloaded from GenBank, as provided in Table 3, using BioEdit version 7.2.5 (Hall 1999) and SeaView version 4.5.2 (Gouy et al. 2010). Bayesian phylogenetic trees were built using MrBayes version 3.2.2 (Ronquist et al. 2012) plugin in Geneious version 8.1. Maximum likelihood phylogenetic trees were built using PhyML version 3.0 (Stamatakis, 2014) plugin in Geneious version 8.1 (Kearse et al. 2012). The model used for the phylogenetic trees is GTR + Γ + I as indicated by Jmodeltest version 2.1.7 (Guindon and Gascuel 2003, Darriba et al. 2012). Distance matrices were built using Geneious version 8.1. *Polysphondylium violaceum* brefeld was used as an outgroup taxon in the molecular phylogenetic trees in Figures 7-8 based on the study by Shaap et al (2006), which indicated that *D. violaceum* is a sister taxon to group four dictyostelids.

Table 3: GenBank accession numbers of nuclear rDNA sequences of dictyostelid species used to construct the molecular phylogenetic trees, with the strain or isolate name (when available).

Dictyostelid Species	Isolate/Strain	GenBank Accession Number	
		SSU rDNA	ITS rDNA
D. aureum L. S. Olive	SL1	AM168028	HQ141449
D. brunneum Kawabe	WS700	AM168031	HQ141451
D. capitatum H. Hagiw	91HO50	AM168032	HQ141452
D. crassicaule H. Hagiw	93HO33	AM168037	HQ141456
D. implicatum H. Hagiw	93HO1	AM168043	HQ141462
D. intermedium Cavender	PJ11	AM168044	HQ141463
D. mucoroides var. stoloniferum	FOII1	AM168055	HQ141469
D. pseudobrefeldianum H. Hagiw	91HO8	AM168059	HQ141470
D. rosarium Raper & Cavender	M45	AM168065	HQ141474
D. septentrionalis Cavender	AK2	AM168067	HQ141476
D. sphaerocephalum	GR11	AM168068	HQ141477
D. mucoroides Bref.	S28b	AM168054	HQ141468
D. clavatum H. Hagiw	TNSC220	AM168035	HQ141455
D. giganteum H. Singh	WS589	AM168042	HQ141461
D. macrocephalum H. Hagiw	B33	AM168049	HQ141465
P. violaceum Bref.	P6	AM168108	HQ732199
D. purpureum	WS321	AM168061	HQ141472
D. purpureum	C143	AM168060	HQ141471
D. purpureum	-	-	AF219103
D. purpureum	Cavender	HQ141481	-
D. purpureum	-	AY040335	-
D. citrinum Vadell	-	DQ340385	
D. discoideum Raper	-	X00601	
D. purpureum	-	DQ340386	
D. purpureum	QSpu37	FJ424827	
D. purpureum	QSpu4	FJ424826	
D. purpureum	QSpu25	FJ424859	
D. purpureum	QSpu27	FJ424835	
D. purpureum	QSpu7	FJ424842	
D. purpureum	QSpu16	FJ424851	
D. purpureum	QSpu3	FJ424840	
D. purpureum	QSpu18	FJ424853	
D. purpureum	QSpu8	FJ424843	
D. purpureum	QSpu28	FJ424836	
D. purpureum	QSpu9	FJ424844	
D. purpureum	QSpu21	FJ424831	
D. purpureum	QSpu1	FJ424829	
D. purpureum	QSpu2	FJ424839	
D. purpureum	QSpu17	FJ424852	
D. purpureum	QSpu23	FJ424832	
D. purpureum	QSpu6	FJ424830	
D. purpureum	QSpu33	FJ424833	
D. purpureum	QSpu30	FJ424838	
D. purpureum	QSpu29	FJ424834	

The outgroup taxa *D. macrocephalum, D. citrinum, and D. discoideum* were used in the molecular phylogenetic trees in Figures 9-14 because they belong to group four dictyostelids based on the study by Schaap et al (2006), and also in order to compare the results to the molecular phylogenetic study of *D. purpureum* conducted by Mehdiabadi et al (2009), in which the same outgroup taxa were used.

Morphological Studies

Morphological studies were performed using images obtained with both a LEICA Z16 APO dissecting microscope, and an Axionscope 2 Plus compound microscope (Carl Zeiss Microscopy Gmbh, Gottingen, Germany). The dissecting microscope is equipped with Lieca cam DFC495 with the supporting software Leica Application Suite version 4.0 (Leica Microsystems, Heerbrugg, Switzland). The compound microscope is equipped with the lenses (10x, 20x, 40x, 50x, and 60x), and a digital camera Canon EOS (Cannon United States, Inc, Melville, New York), with the supporting software EOS utility version 2.14.1. All measurements were made using Auto-Montage Pro version 5.03.0061 (Syncroscopy, Cambridge, United Kingdom) and ImageJ version 1.45s.

For spore measurements, plates of the different isolates were subcultured from silica gel tubes for one week. From each plate, several sori were suspended in 300 µl of distilled water using an inoculation loop. The concentration of each spore suspension was determined using a hemocytometer, and further diluted to a concentration of 5×10^4 spores per ml. Two hundred µl of the diluted spores from each isolate were mixed with 40 µl of *E. coli* suspension, and spread on low nutrient agar plates using a sterile glass spreader. The experiment was duplicated for each isolate. The plates were maintained under controlled light conditions (12 hours light, 12 hours dark) at a temperature of 21.5 °C. The plates were observed for the following two to three weeks.

Images of the spores were taken on day 10, by mounting several sori in distilled water on a slide using the compound microscope, and around 30 spores were measured for each isolate. Other morphological features such as growth habit, aggregation pattern, sorus color, branching pattern, migration, and macrocyst formation were observed directly on the agar plates, using both dissecting and compound microscopes.

The phototropism characteristic of each isolate was tested by growing the isolates under a directional source of light. The isolates were grown on agar plates that were fully covered with aluminium foil, except for a small part at the side of the plates to allow the light to enter.

Mating Experiments

Mating experiments and determination of macrocyst formation for each combination of the different isolates were performed following the method described in the literature, with several variations (Nickerson and Raper 1973, Lewis and O'Day 1976). Each pair of isolates was cultured on the same plate (0.1% lactose, 0.1% peptone agar plates) at 21.5 °C under dark conditions, with or without the addition of 0.5 milliliter of Bonner's salt solution (Bonner and Savage 1947). For underwater growth, spores and *E. coli* were mixed in 5 milliliter of Bonner's salt solution and poured on the agar plates. Moreover, each isolate was cultured separately to infer whether the isolate is homothallic and thus able to produce macrocysts by itself.

Results

Molecular Data

The ITS1, ITS2, and 5.8S sequences were obtained for all of the 11 studied isolates in both directions. For the SSU rDNA,~1200 bp sequences were obtained for nine of the isolates using the four primers mentioned in the Materials and Methods in both directions. However,~500 bp of the SSU rDNA flanking regions from two single primers were also used to build the molecular phylogenetic trees. Bayesian and maximum likelihood trees based on 5.8S and SSU rDNA are provided in Figures 7-14. Maximum likelihood and Bayesian phylogenetic trees indicate that *D. purpureum* isolates comprise a clade within group four of dictyostelids, as shown in Figures 7-8. The 18S rDNA and the combined 18S and 5.8S rDNA molecular phylogenetic trees of the studied isolates provided in Table 2 indicate the presence of three groups, named A', B', and C', but with low support for the groups B' and C', as shown in Figure 9. The topology of the molecular trees based on18S rDNA and the combined 18S and 5.8S rDNA molecular phylogenetic trees in Figure 12 and Figure 14 shows the presence of three groups within *D. purpureum* named A, B, and C, while Isolates NB1B 2271 and C143 are located in different branches, and are labeled with the letters D and E respectively. Distance matrices for the 5.8S and SSU rDNA sequences of 16 dictyostelid isolates are provided in Tables 4-5. In the multiple sequence alignment of the ITS rDNA regions, it is noted that ITS rDNA sequences are not alignable within all group four dictyostelid species, or among all the isolates of *D. purpureum*. However, within the different groups A, B and C, ITS rDNA regions are alignable. Isolates NB1B 2271 and C143 are not alignable with any of the isolates of *D. purpureum.*

Morphological Data

The 11 studied isolates of *D. purpureum* share the similar morphological characteristics listed below:

- Solitary growth without lateral branches.
- Aggregation toward the center in streams, and slug migration after stalk formation.
- Elliptical spores without polar granules.
- Positive phototropic response.

All the studied isolates have a light brown/purple color sori that becomes darker when they mature, except for the isolates M8B and MK11B 2522 that have a gray color sori that turns to black when mature. Images that illustrate the life cycle stages of *D. purpureum* are provided in Figure 15. Image of slug migration of one isolate MK11B 2522 toward a directional light source is provided in Figure 16. Spore dimensions of the studied isolates of *D. purpureum* are shown in Figures 17-19.

Mating Results and Macrocysts Formation

Positive mating results and macrocysts formation were observed only in the homothallic strains of *D. purpureum*, Za2a OH216 and TRII-1 OH278, and no positive heterothallic mating results were observed. Isolate Za2a OH216 produces more macrocysts than isolate TRII-1 OH278. Moreover, it was noted that under dark conditions, and in the absence of charcoal, macrocysts formation was more intense and faster than under light conditions, or in the presence of charcoal. Image of macrocysts of isolate Za2a OH216 is provided in Figure 20.

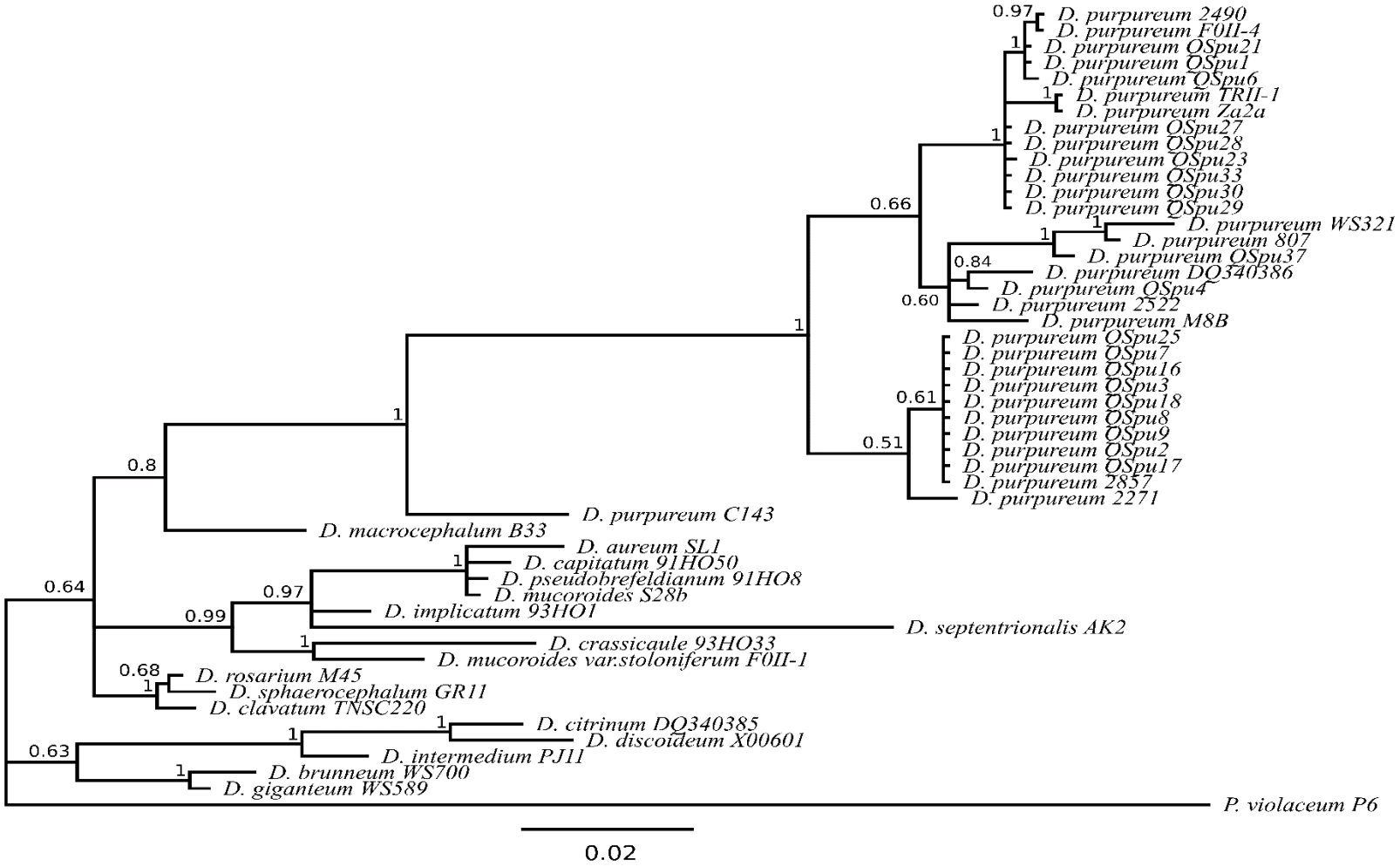

Figure 7. Bayesian phylogenetic analyses based on 1876 unambiguously aligned sites of 49 combined 5.8S and SSU rDNA group four dictyostelid sequences, together with *Polysphondylium violaceum* as an outgroup taxon. The tree was built using MrBayes version 3.2.2 (Ronquist et al. 2012) plugin in Geneious version 8.1 (Kearse et al. 2012) utilizing a GTR + Γ + I model as suggested by jModelTest 2.1.7 (Guindon and Gascuel 2003, Darriba et al. 2012). Bayesian inference posterior probabilities are shown on the branches.

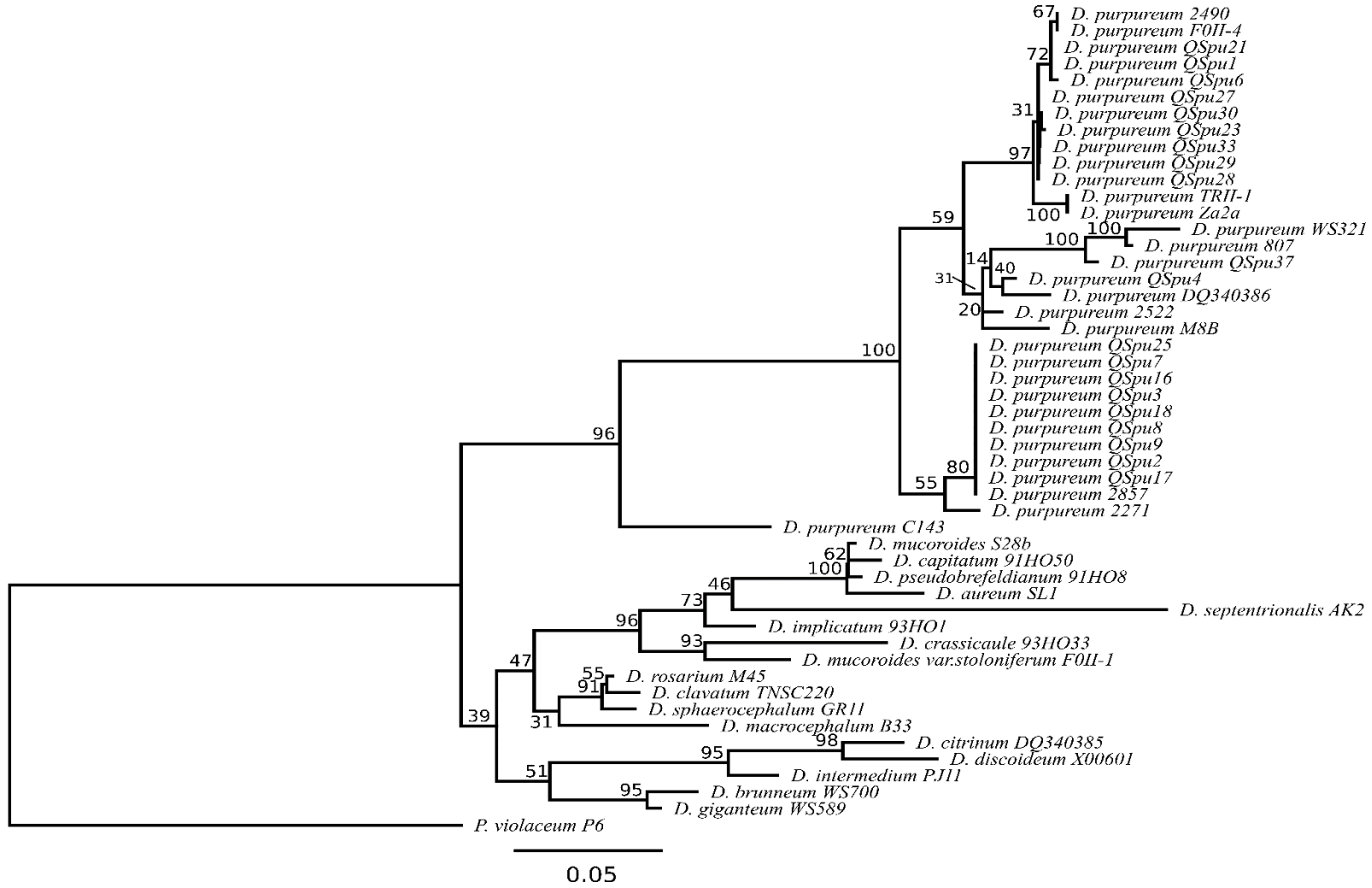

Figure 8. Maximum likelihood tree based on 1876 unambiguously aligned sites of 49 combined 5.8S and SSU rDNA group four dictyostelid sequences, together with *Polysphondylium violaceum* as an outgroup taxon. The tree was built using PhyML version 3.0 (Stamatakis, 2014) plugin in Geneious version 8.1 (Kearse et al. 2012) utilizing a GTR + Γ + I model as suggested by jModelTest 2.1.7 (Guindon and Gascuel 2003, Darriba et al. 2012). Maximum likelihood bootstrap support values are shown on the branches.

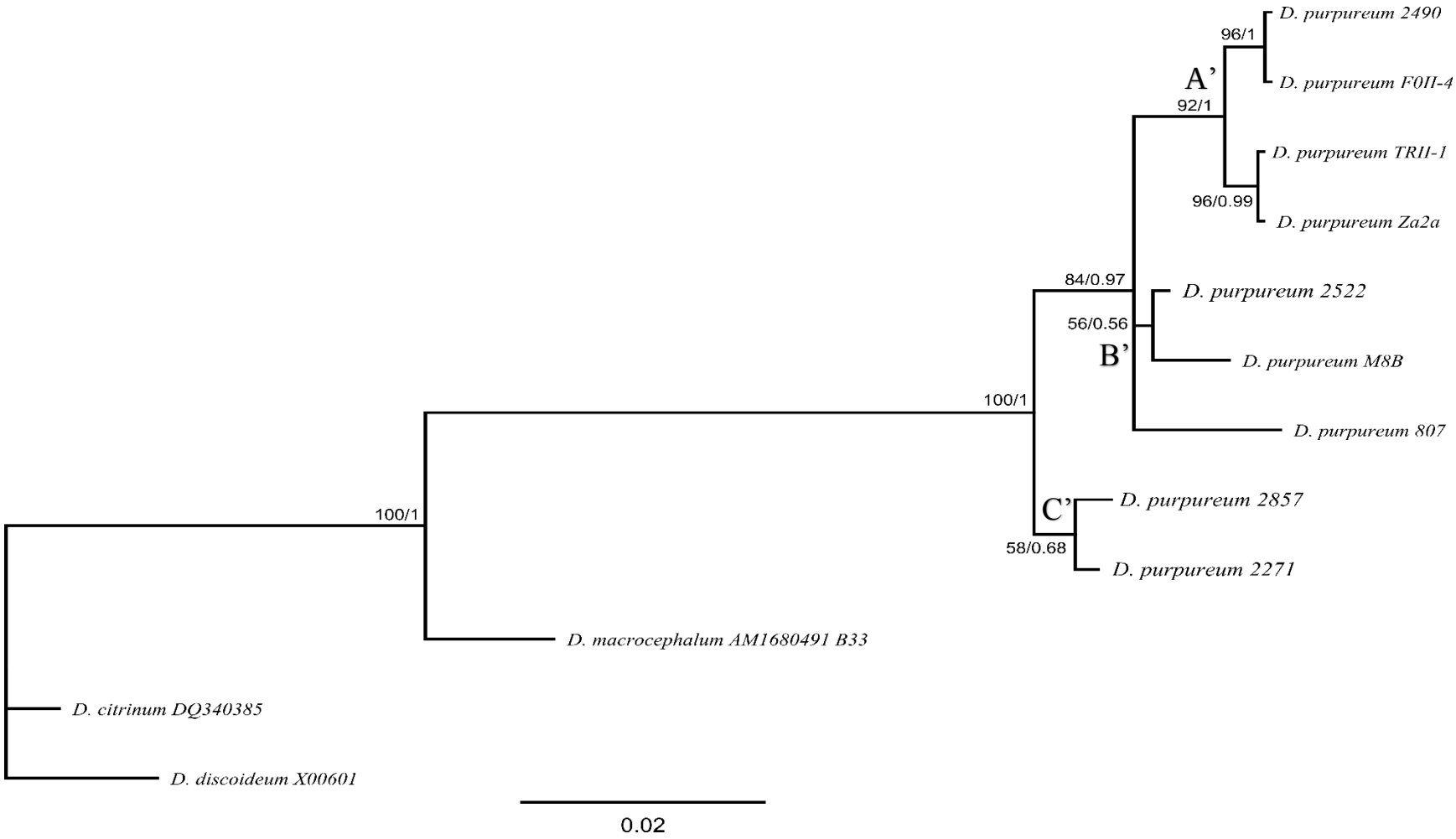

Figure 9. Bayesian phylogenetic analyses based on 1651 unambiguously aligned sites of 9 SSU rDNA *D. purpureum* sequences, together with *D. macrocephalum, D. citrinum, and D. discoideum* as an outgroup taxa. The tree was built using MrBayes version 3.2.2 (Ronquist et al. 2012) plugin in Geneious version 8.1 (Kearse et al. 2012) utilizing a GTR + Γ + I model as suggested by jModelTest 2.1.7 (Guindon and Gascuel 2003, Darriba et al. 2012). Maximum likelihood bootstrap support and Bayesian inference posterior probabilities are shown on the branches to the left and right of the slash sign, respectively.

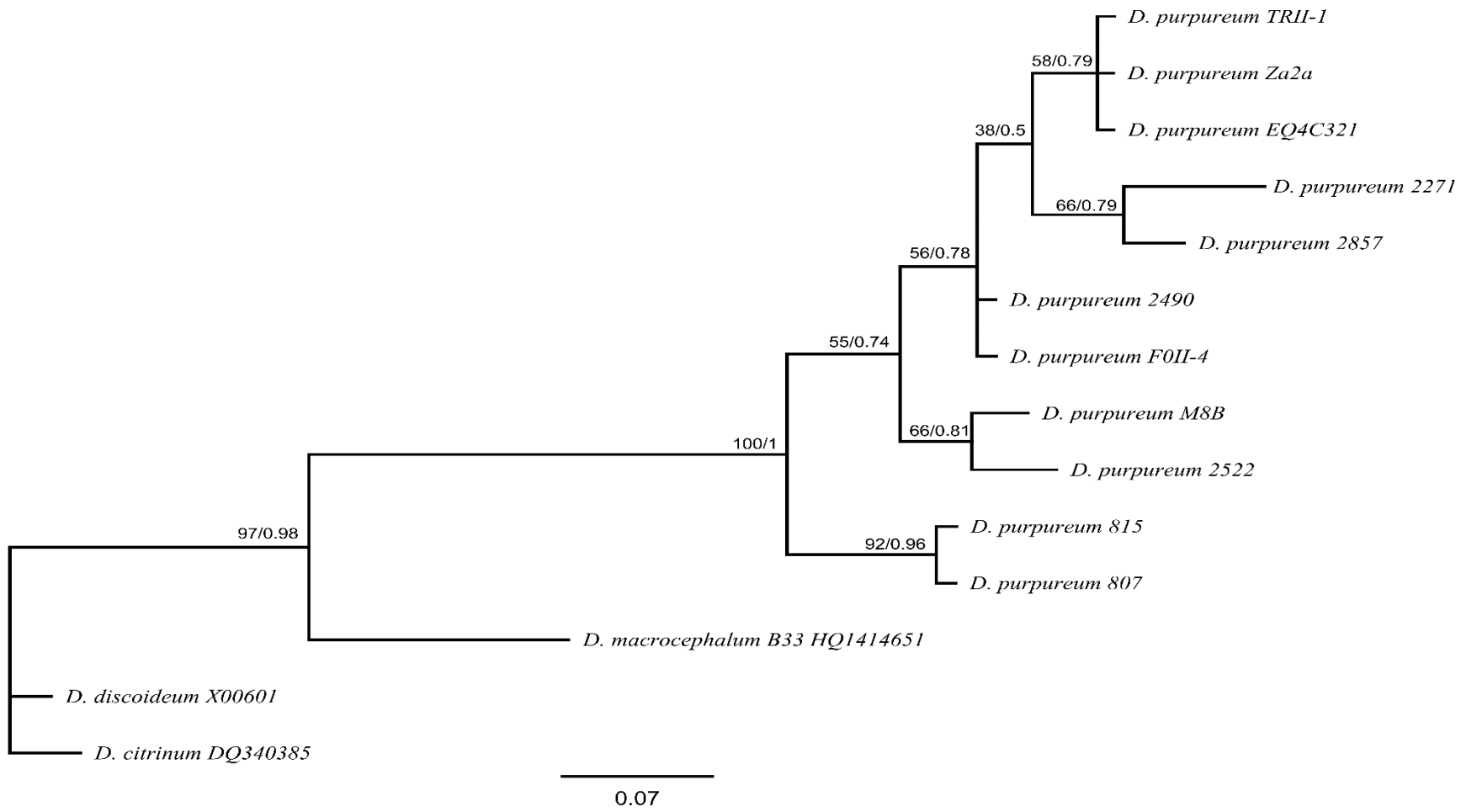

Figure 10. Bayesian phylogenetic analyses based on 225 unambiguously aligned sites of 11 5.8S *D. purpureum* sequences, together with *D. macrocephalum, D. citrinum, and D. discoideum* as an outgroup taxa. The tree was built using MrBayes version 3.2.2 (Ronquist et al. 2012) plugin in Geneious version 8.1 (Kearse et al. 2012) utilizing a GTR + Γ + I model as suggested by jModelTest 2.1.7 (Guindon and Gascuel 2003, Darriba et al. 2012). Maximum likelihood bootstrap support and Bayesian inference posterior probabilities are shown on the branches to the left and right of the slash sign, respectively.

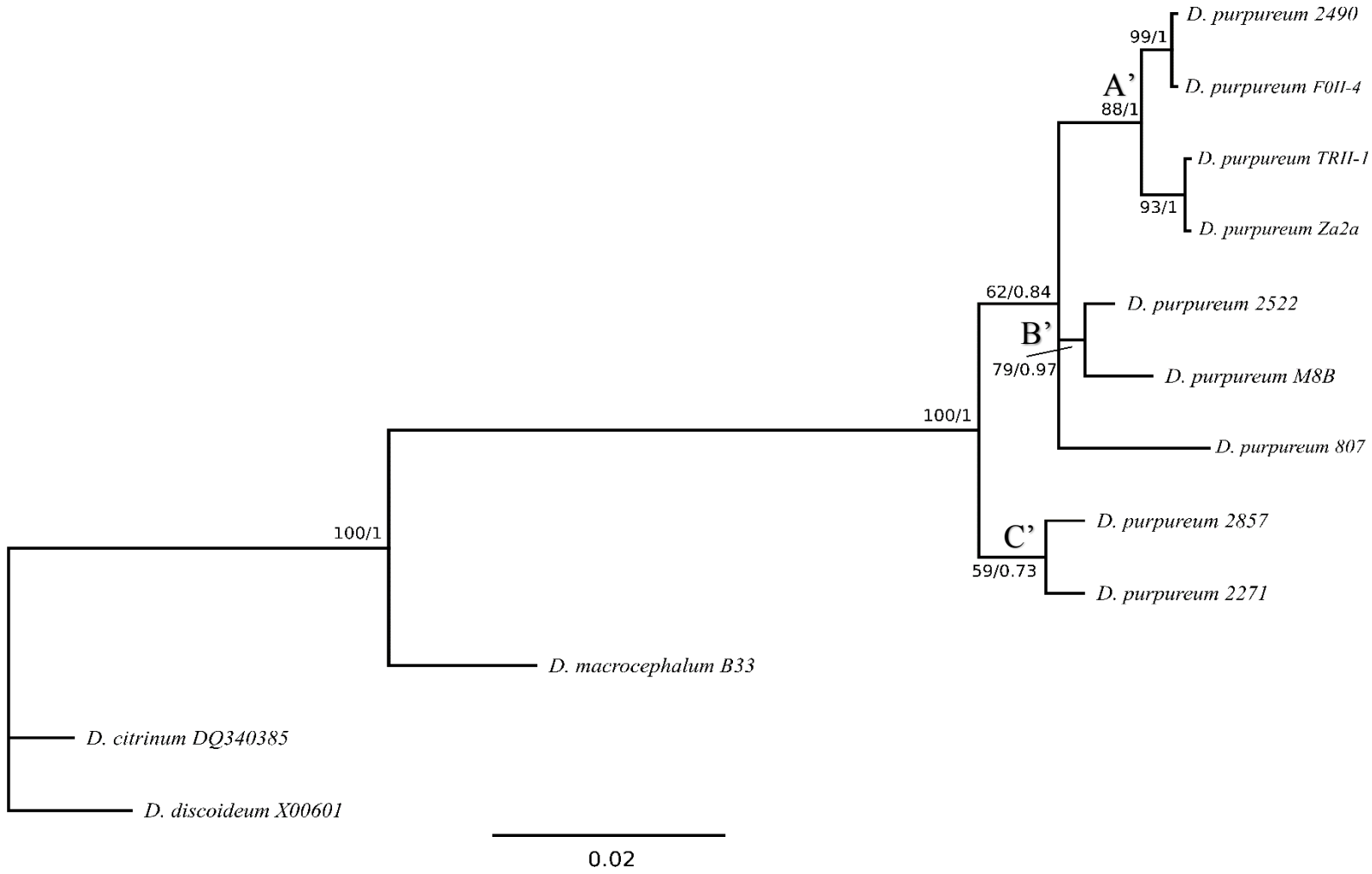

Figure 11. Bayesian phylogenetic analyses based on 1876 unambiguously aligned sites of 9 combined 5.8S and SSU rDNA of *D. purpureum* sequences, together with *D. macrocephalum, D. citrinum, and D. discoideum* as an outgroup taxa. The tree was built using MrBayes version 3.2.2 (Ronquist et al. 2012) plugins in Geneiou version 8.1 (Kearse et al. 2012) utilizing a GTR + Γ + I model as suggested by jModelTest 2.1.7 (Guindon and Gascuel 2003, Darriba et al. 2012). Maximum likelihood bootstrap support and Bayesian inference posterior probabilities are shown on the branches to the left and right of the slash sign, respectively.

Figure 12. Bayesian phylogenetic analyses based on 1651 unambiguously aligned sites of 34 SSU rDNA *D. purpureum* sequences, together with *D. macrocephalum, D. citrinum, and D. discoideum* as an outgroup taxa. The tree was built using MrBayes version 3.2.2 (Ronquist et al. 2012) plugin in Geneious version 8.1 (Kearse et al. 2012) utilizing a GTR + Γ + I model as suggested by jModelTest 2.1.7 (Guindon and Gascuel 2003, Darriba et al. 2012). Maximum likelihood bootstrap support and Bayesian inference posterior probabilities are shown on the branches to the left and right of the slash sign, respectively. The studied isolates provided in Table 2 are labeled with a star (★).

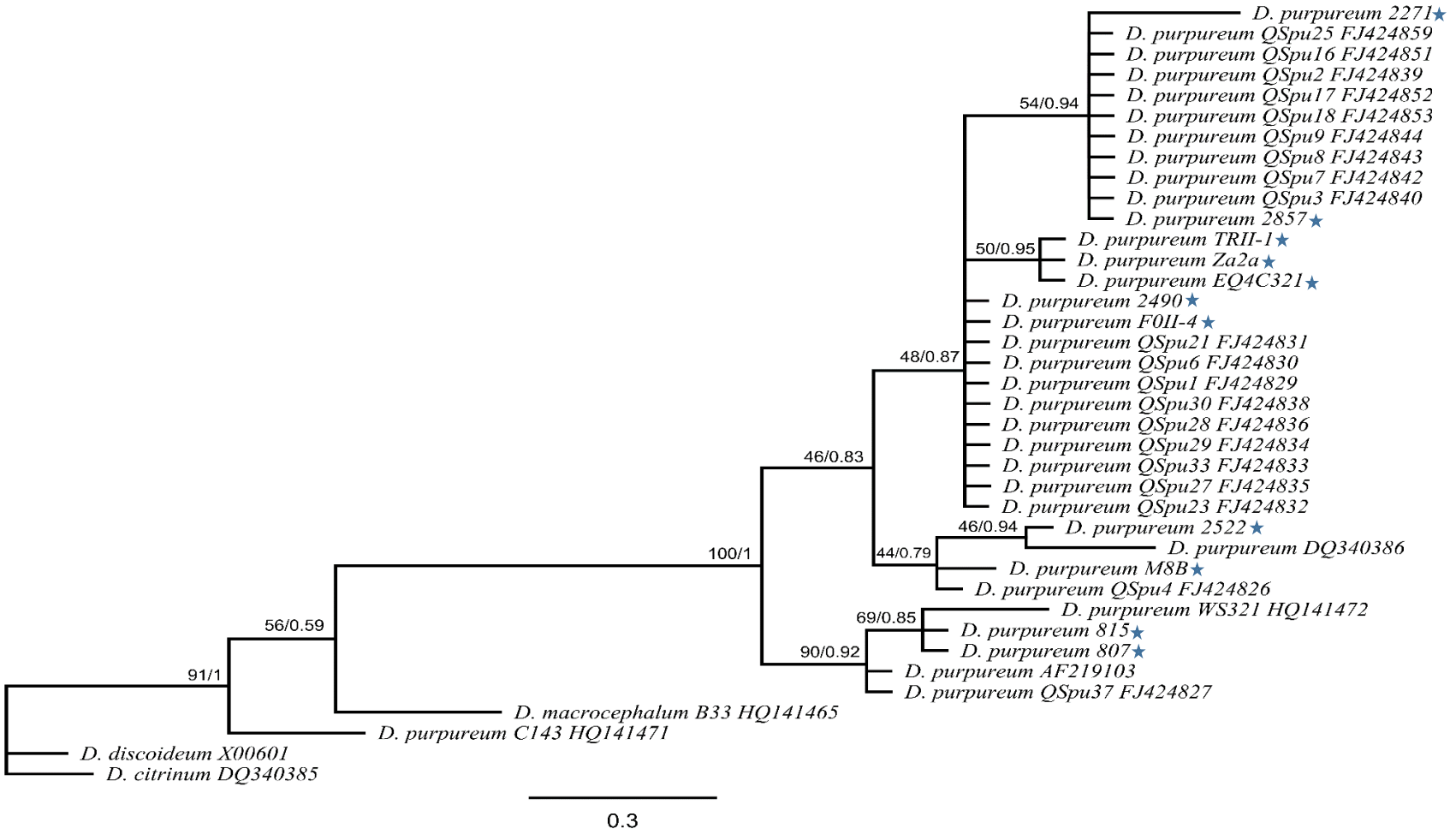

Figure 13. Bayesian phylogenetic analyses based on 225 unambiguously aligned sites of 35 5.8S *D. purpureum* sequences, together with *D. macrocephalum, D. citrinum, and D. discoideum* as an outgroup taxa. The tree was built using MrBayes version 3.2.2 (Ronquist et al. 2012) plugin in Geneious version 8.1 (Kearse et al. 2012) utilizing a GTR + Γ + I model as suggested by jModelTest 2.1.7 (Guindon and Gascuel 2003, Darriba et al. 2012). Maximum likelihood bootstrap support and Bayesian inference posterior probabilities are shown on the branches to the left and right of the slash sign, respectively. The studied isolates provided in Table 2 are labeled with a star (★).

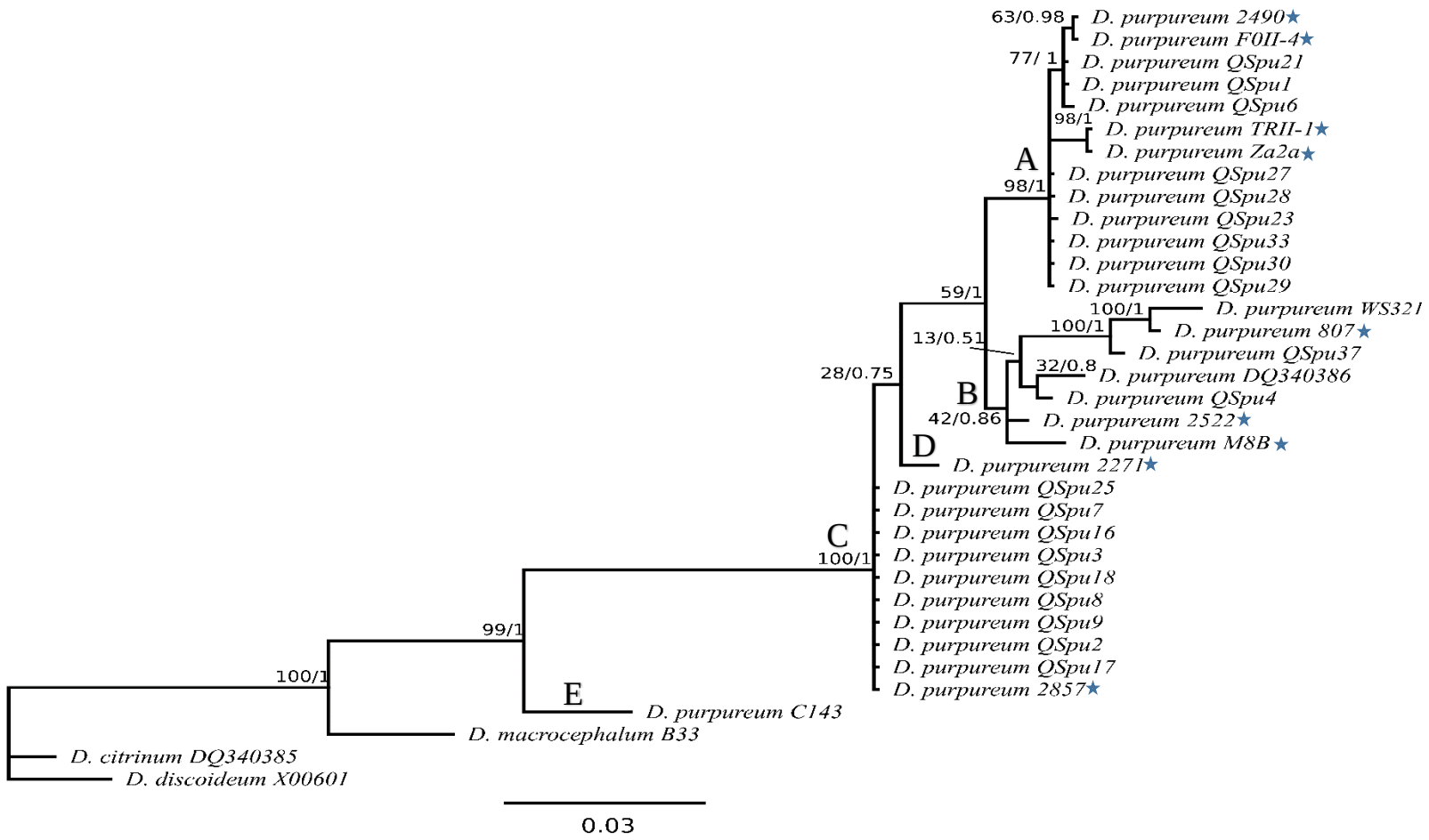

Figure 14. Bayesian phylogenetic analyses based on 1876 unambiguously aligned sites of 32 combined 18S and 5.8S *D. purpureum* sequences, together with *D. macrocephalum, D. citrinum, and D. discoideum* as an outgroup taxa. The tree was built using MrBayes version 3.2.2 (Ronquist et al. 2012) plugin in Geneious version 8.1 (Kearse et al. 2012) utilizing a GTR + Γ + I model as suggested by jModelTest 2.1.7 (Guindon and Gascuel 2003, Darriba et al. 2012). Maximum likelihood bootstrap support and Bayesian inference posterior probabilities are shown on the branches to the left and right of the slash sign, respectively. The studied isolates provided in Table 2 are labeled with a star (★).

Table 4. Distance-matrix of 1651 aligned SSU rDNA sites of 16 dictyostelid species. The matrix was built using Geneious version 8.1 (Kearse et al. 2012). Numbers are percent of identity.

	D. purpureum 2490	***D. purpureum QSpu6***	***D. purpureum TRII-1***	***D. purpureum QSpu27***	***D. purpureum QSpu29***	***D. purpureum WS321***	***D. purpureum QSpu4***	***D. purpureum 2522***	***D. purpureum M8B***	***D. purpureum QSpu25***	***D. purpureum QSpu17***	***D. purpureum 2857***	***D. purpureum 2271***	***D. purpureum C143***	***D. macrocephalum B33***	***D. Citrinum DQ340385***
D. purpureum 2490		99.9	99.5	99.7	99.8	97.7	98.8	99.0	98.6	98.3	98.3	98.3	98.1	96.5	95.3	94.2
D. purpureum QSpu6	99.9		99.6	99.8	99.9	97.7	98.8	99.1	98.6	98.3	98.3	98.3	98.2	96.6	95.4	94.3
D. purpureum TRII-1	99.5	99.6		99.6	99.7	97.7	98.8	99.1	98.5	98.1	98.1	98.1	98.0	96.4	95.2	94.1
D. purpureum QSpu27	99.7	99.8	99.6		99.9	97.9	99.0	99.1	98.6	98.4	98.4	98.4	98.3	96.6	95.3	94.1
D. purpureum QSpu29	99.8	99.9	99.7	99.9		97.8	98.9	99.2	98.8	98.4	98.4	98.4	98.3	96.6	95.3	94.1
D. purpureum WS321	97.7	97.7	97.7	97.9	97.8		98.5	98.4	97.9	97.9	97.9	97.9	97.7	96.3	95.1	93.7
D. purpureum QSpu4	98.8	98.8	98.8	99.0	98.9	98.5		99.4	98.9	98.5	98.5	98.5	98.4	97.2	95.3	94.4
D. purpureum 2522	99.0	99.1	99.1	99.1	99.2	98.4	99.4		99.4	98.6	98.6	98.6	98.6	96.7	95.4	94.5
D. purpureum M8B	98.6	98.6	98.5	98.6	98.8	97.9	98.9	99.4		98.4	98.4	98.4	98.3	96.3	95.3	94.5
D. purpureum QSpu25	98.3	98.3	98.1	98.4	98.4	97.9	98.5	98.6	98.4		100	100	99.5	97.1	95.7	94.5
D. purpureum QSpu17	98.3	98.3	98.1	98.4	98.4	97.9	98.5	98.6	98.4	100		100	99.5	97.1	95.7	94.5
D. purpureum 2857	98.3	98.3	98.1	98.4	98.4	97.9	98.5	98.6	98.4	100	100		99.5	97.1	95.7	94.5
D. purpureum 2271	98.1	98.2	98.0	98.3	98.3	97.7	98.4	98.6	98.3	99.5	99.5	99.5		96.8	95.7	94.4
D. purpureum C143	96.5	96.6	96.4	96.6	96.6	96.3	97.2	96.7	96.3	97.1	97.1	97.1	96.8		96.6	95.0
D. macrocephalum B33	95.3	95.4	95.2	95.3	95.3	95.1	95.3	95.4	95.3	95.7	95.7	95.7	95.7	96.6		96.3
D. citrinum DQ340385	94.2	94.3	94.1	94.1	94.1	93.7	94.4	94.5	94.5	94.5	94.5	94.5	94.4	95.0	96.3	

Table 5. Distance-matrix of 225 aligned 5.8S rDNA sites of 16 dictyostelid species. The matrix was built using Geneious version 8.1 (Kearse et al. 2012). Numbers are percent identity.

	D. purpureum 2490	***D. purpureum QSpu6***	***D. purpureum TRII-1***	***D. purpureum QSpu27***	***D. purpureum QSpu29***	***D. purpureum WS321***	***D. purpureum QSpu4***	***D. purpureum 2522***	***D. purpureum M8B***	***D. purpureum QSpu25***	***D. purpureum QSpu17***	***D. purpureum 2857***	***D. purpureum 2271***	***D. purpureum C143***	***D. macrocephalum B33***	***D. Citrinum DQ340385***
D. purpureum 2490		100	99.1	100	100	95.3	98.6	97.7	97.7	98.1	98.1	98.1	96.7	91.1	92.1	87.0
D. purpureum QSpu6	100		99.1	100	100	95.3	98.6	97.7	97.7	98.1	98.1	98.1	96.7	91.1	92.1	87.0
D. purpureum TRII-1	99.1	99.1		99.1	99.1	94.4	97.7	97.2	96.7	98.1	98.1	98.1	97.2	90.7	91.1	87.0
D. purpureum QSpu27	100	100	99.1		100	95.3	98.6	97.7	97.7	98.1	98.1	98.1	96.7	91.1	92.1	87.0
D. purpureum QSpu29	100	100	99.1	100		95.3	98.6	97.7	97.7	98.1	98.1	98.1	96.7	91.1	92.1	87.0
D. purpureum WS321	95.3	95.3	94.4	95.3	95.3		95.8	94.9	94.9	94.4	94.4	94.4	93.9	90.2	91.1	86.1
D. purpureum QSpu4	98.6	98.6	97.7	98.6	98.6	95.8		99.1	99.1	97.7	97.7	97.7	96.3	91.6	92.5	87.4
D. purpureum 2522	97.7	97.7	97.2	97.7	97.7	94.9	99.1		98.1	96.7	96.7	96.7	95.8	91.6	92.5	87.4
D. purpureum M8B	97.7	97.7	96.7	97.7	97.7	94.9	99.1	98.1		96.7	96.7	96.7	95.3	92.1	92.1	87.9
D. purpureum QSpu25	98.1	98.1	98.1	98.1	98.1	94.4	97.7	96.7	96.7		100	100	97.7	92.1	92.1	87.9
D. purpureum QSpu17	98.1	98.1	98.1	98.1	98.1	94.4	97.7	96.7	96.7	100		100	97.7	92.1	92.1	87.9
D. purpureum 2857	98.1	98.1	98.1	98.1	98.1	94.4	97.7	96.7	96.7	100	100		97.7	92.1	92.1	87.9
D. purpureum 2271	96.7	96.7	97.2	96.7	96.7	93.9	96.3	95.8	95.3	97.7	97.7	97.7		91.6	91.6	87.4
D. purpureum C143	91.1	91.1	90.7	91.1	91.1	90.2	91.6	91.6	92.1	92.1	92.1	92.1	91.6		96.3	92.4
D. macrocephalum B33	92.1	92.1	91.1	92.1	92.1	91.1	92.5	92.5	92.1	92.1	92.1	92.1	91.6	96.3		90.1
D. citrinum DQ340385	87.0	87.0	87.0	87.0	87.0	86.1	87.4	87.4	87.9	87.9	87.9	87.9	87.4	92.4	90.1	

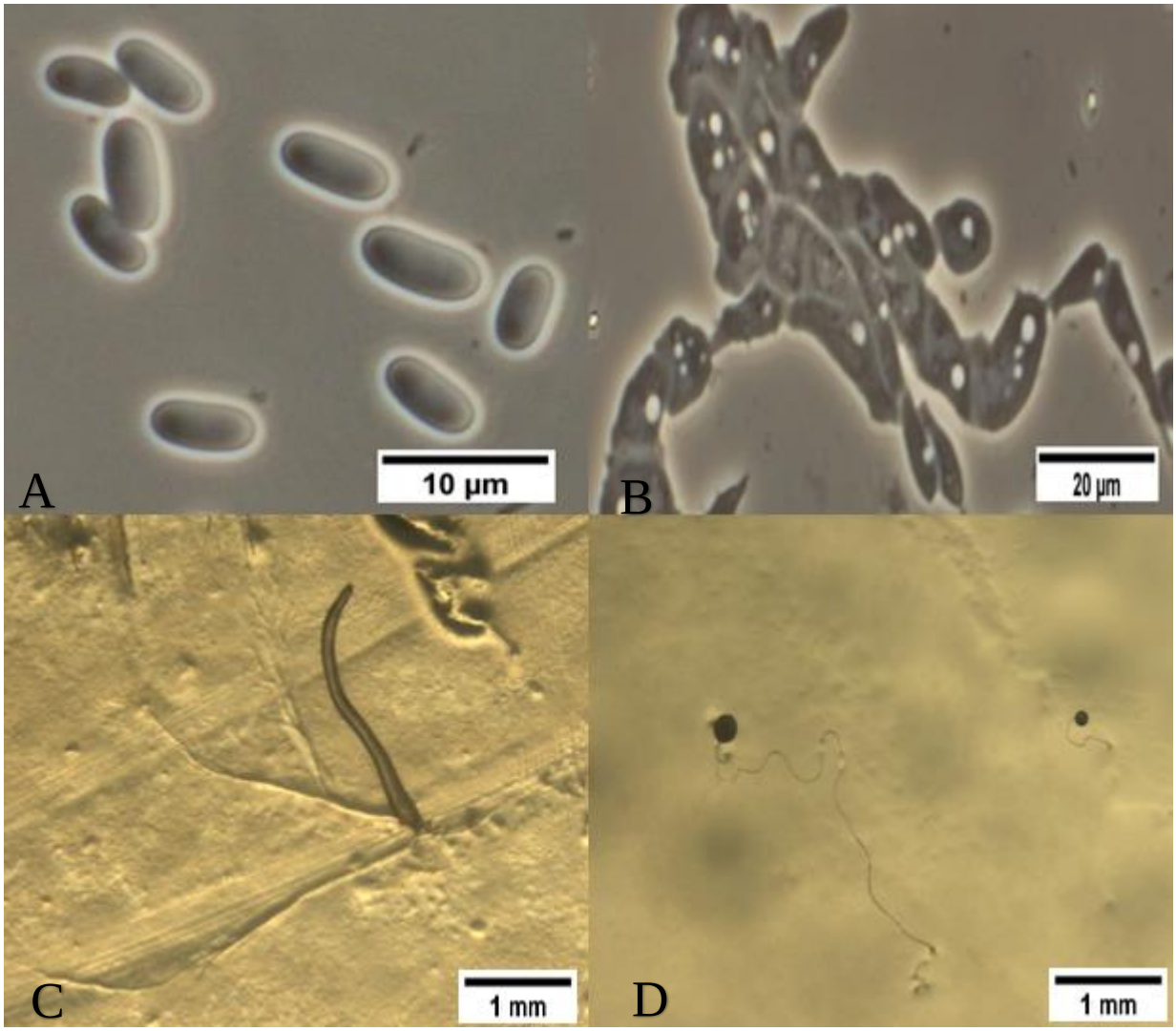

Figure 15. Asexual life cycle of *Dicyostelium purpureum*, isolate MK11B 2522. A. Spores. B. Amoebae. C. Aggregation with early formation of sorogen. D. Sorocarps.

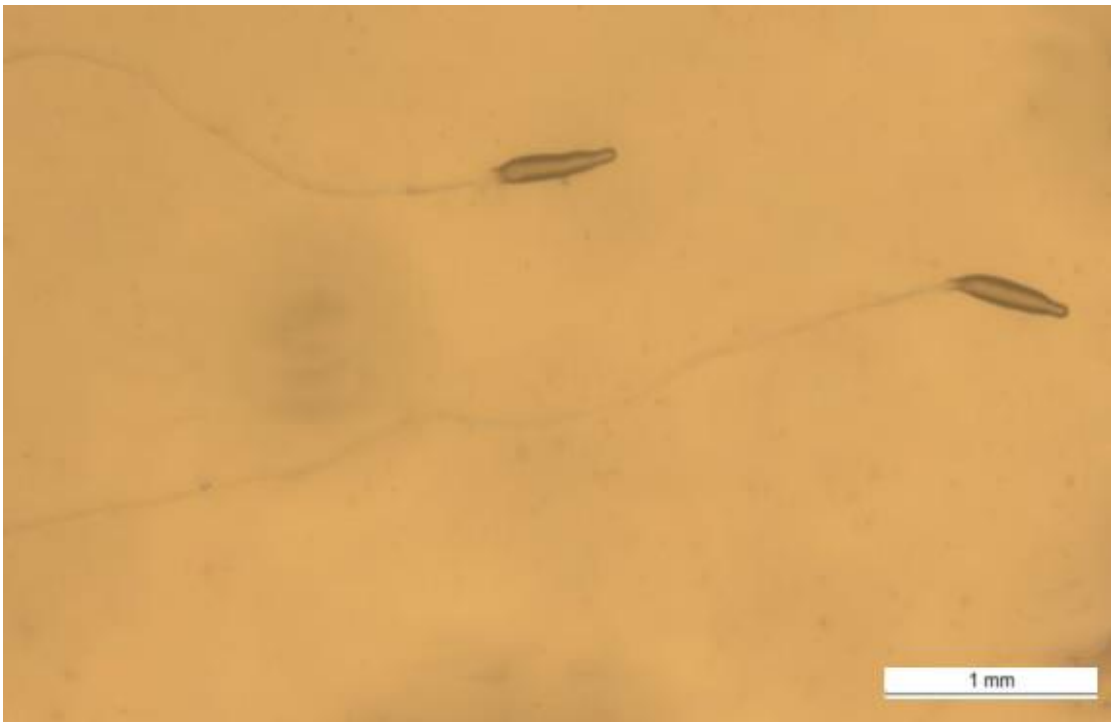

Figure 16. *Dictyostelium purpureum* isolate MK11B 2522 migration toward the light source.

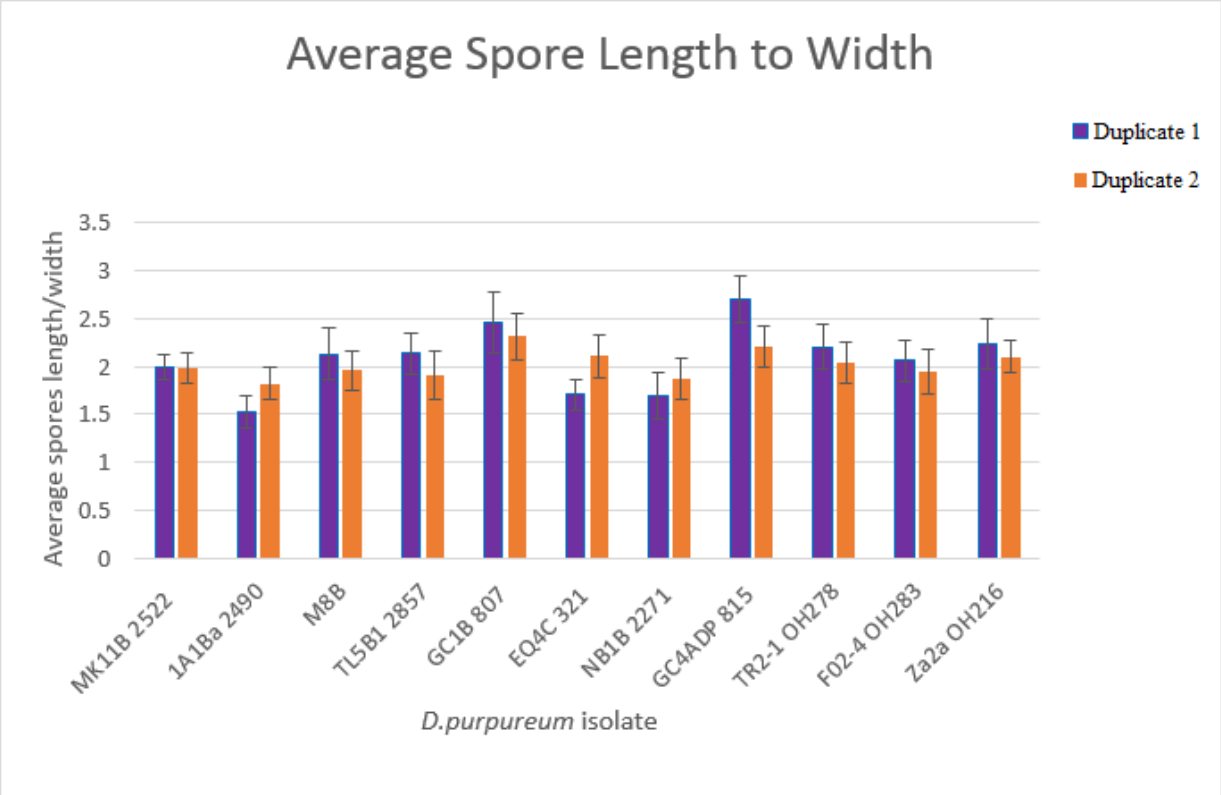

Figure 17. Average spore length to width in duplicate for Isolates of *Dictyostelium purpureum*.

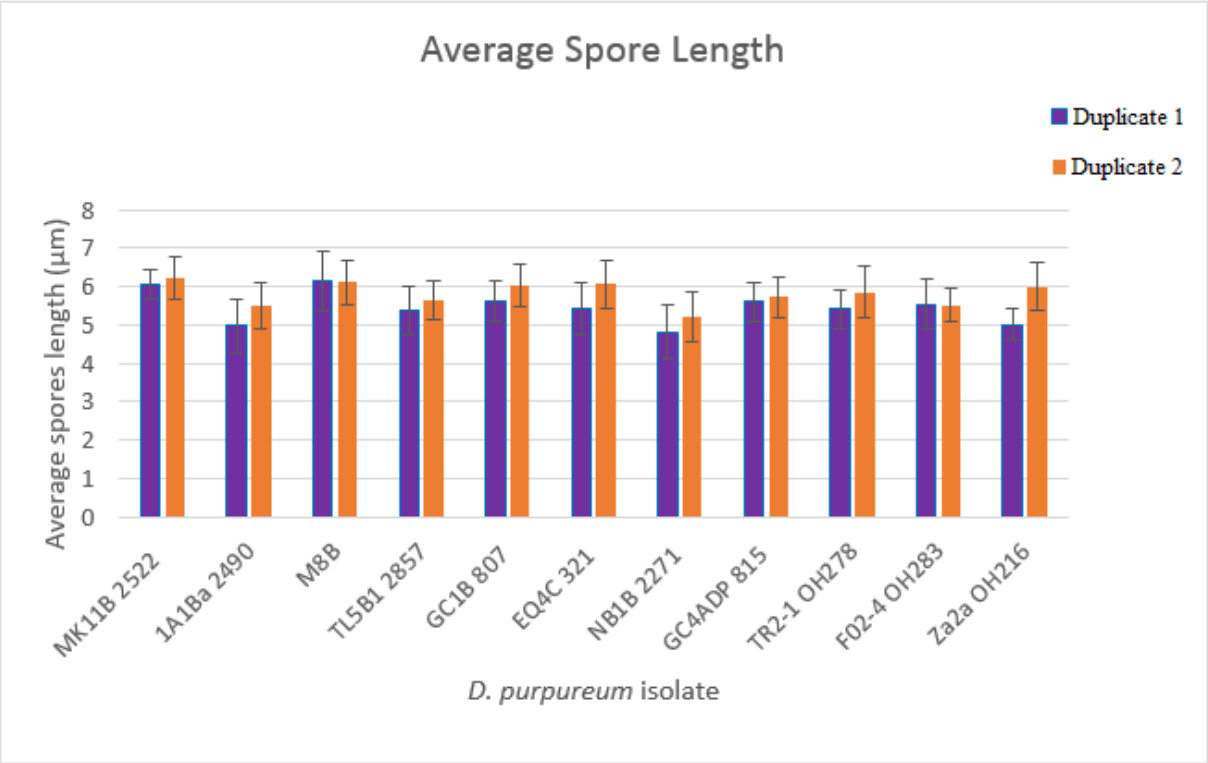

Figure 18. Average spore length (µm) in duplicate for isolates of *Dictyostelium purpureum*.

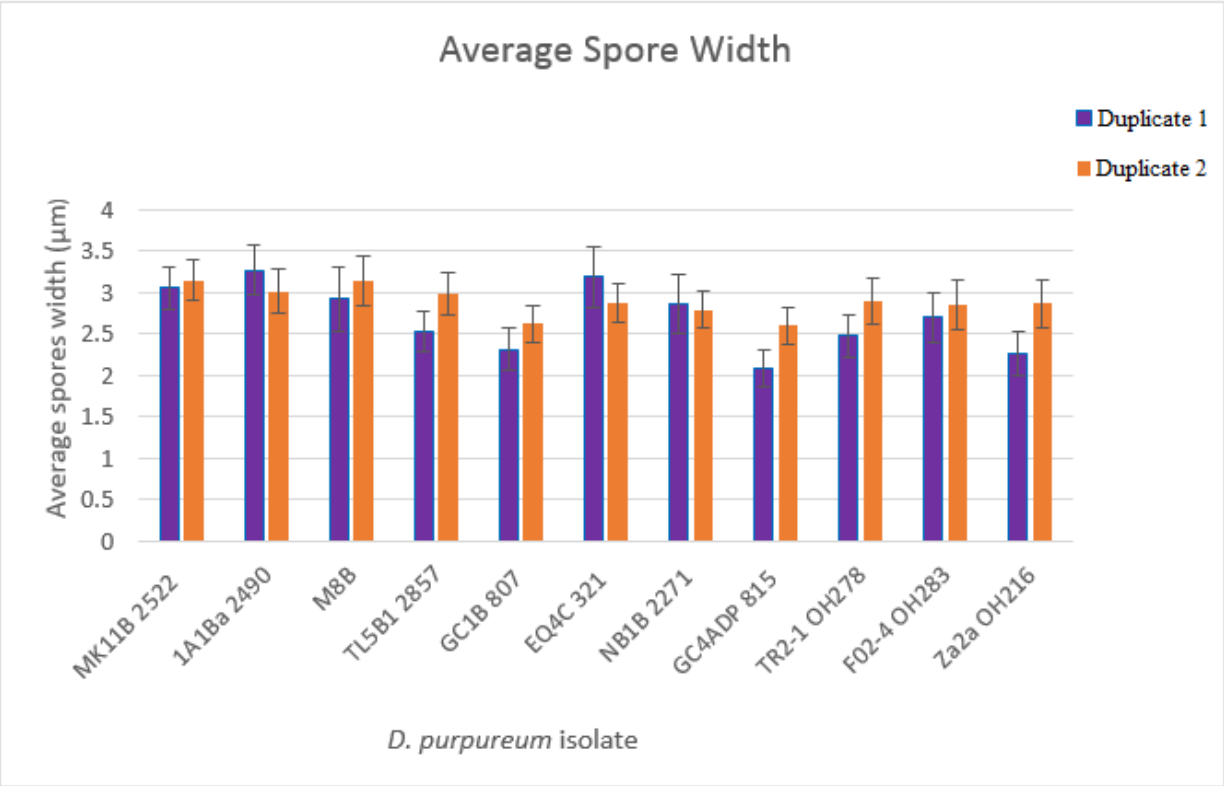

Figure 19. Average spore width (µm) in duplicate for isolates of *Dictyostelium purpureum*.

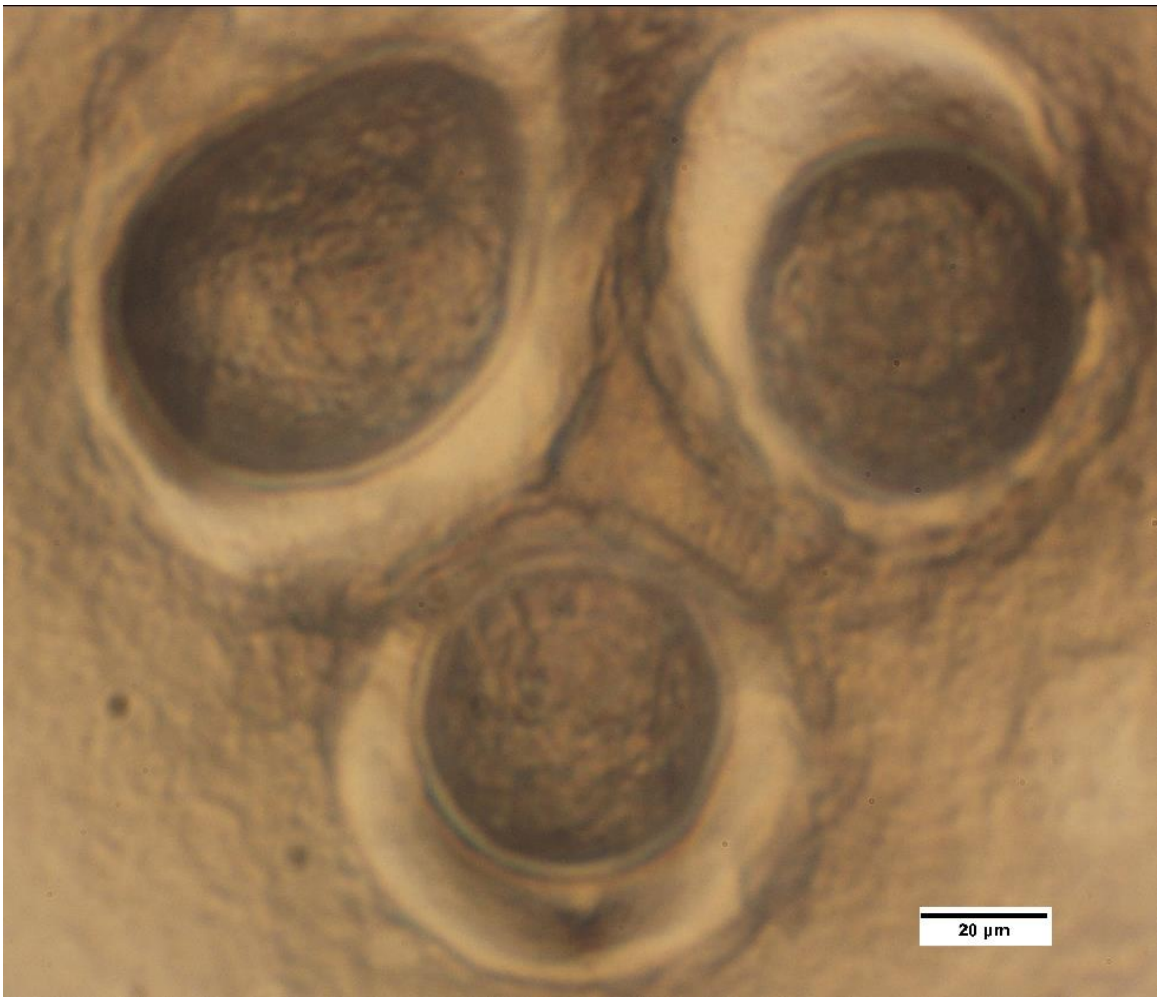

Figure 20. Macrocysts of *Dictyostelium purpureum*, isolate Za2a OH216.

Discussion

Dictyostelid classification was previously based on morphological studies, with the main three groups being *Dictyostelium*, *Polyspondilium* and *Actyostelium*. This classification was changed with the advent of molecular tools into four major groups that do not correspond to the previous morphological ones (Shaap et al. 2006). Further molecular studies focused on the internal phylogeny within the different species while using molecular phylogenetics, morphological studies, and mating tests.

Dictyostelium purpureum is classified within group four of dictyostelids, as shown in Figure 21 (Schaap et al. 2006). The starting point of the internal molecular phylogenetic study of *D. purpureum* was the molecular phylogenetic tree of isolates of *D. purpureum* constructed by Mehdiabadi et al. (2009), as provided in Figure 6. This tree implies that *D. purpureum* isolates comprise three distinct groups named A, B, and C. The tree was constructed based on ~ 4000 bp of nuclear rDNA sequences of 21 haplotypes of *D. purpureum* (Mehdiabadi et al. 2009).

First, to infer whether isolates of *D. purpureum* comprise a clade within group four of dictyoselids, molecular phylogenetic trees were constructed based on combined 18S and 5.8S rDNA sequences of group four isolates downloaded from GenBank and provided in Table 3, together with the sequences of the studied isolates of *D. purpureum* provided in Table 2, as shown in Figures 7-8. It can be noted that isolates of *D. purpureum* form a clade within group four of dictyostelids with strong support (1.00 Bayesian posterior probabilities (bpp) and 96% maximum likelihood bootstrap (ml bs)).

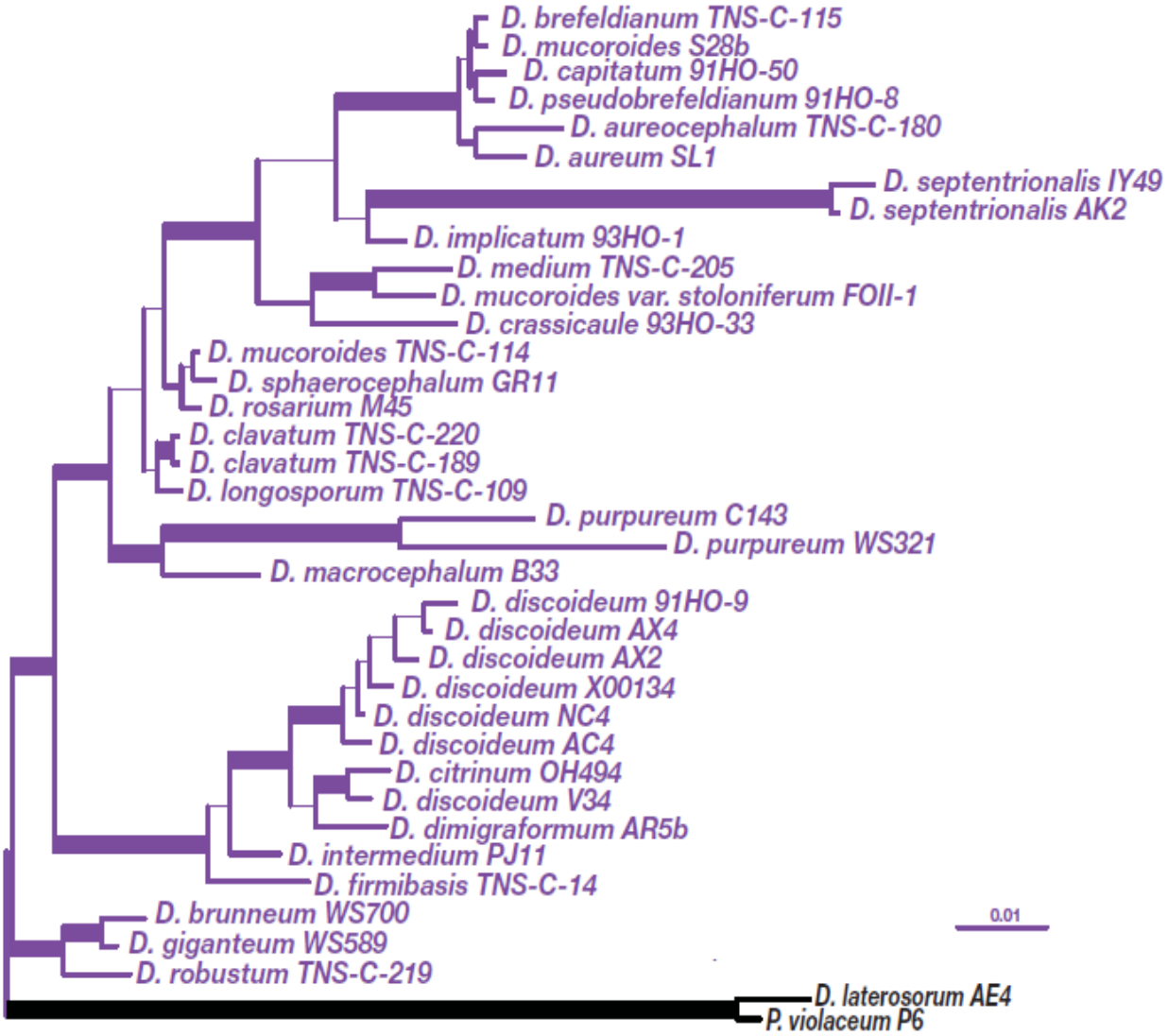

Figure 21. Bayesian phylogenetic analysis based on SSU rDNA sequences of dictyostelids group four isolates, adapted and modified from Schaap et al. (2006). © Reproduced with permission of the publisher, The American Association for the Advancement of Science, 2015.

Second, molecular phylogenetic trees were constructed based on sequences of the studied isolates from Table 2, and sequences of the same outgroups that were used in Mehdiabadi et al. (2009), as seen in Figures 9-11. Three groups with various support values can be noted in the trees constructed using 18S rDNA and the combined 18S and 5.8S rDNA, named A', B', and C'. There is high support for group A' (1.00 bpp and ≥88% ml bs) and the node that separates group C' from the rest of the groups (1.00 bpp and 100% ml bs). The 5.8S rDNA based molecular phylogenetic tree also shows the presence of several groups.

Third, molecular phylogenetic trees were constructed using sequences of the studied isolates provided in Table 2, sequences of *D. purpureum* isolates obtained from GenBank, and sequences of the same outgroups that were used in Mehdiabadi et al. (2009), as shown in Figures 12-14. As expected, in the 18S rDNA and the combined 18S and 5.8S rDNA trees, it can be noted that the groups A, B, and C, reported by Mehdiabadi et al. (2009), are retained, with high support for the groups A and C (1:00 bpp and ≥ 96% ml bs). Isolate NB1B 2271 is a sister taxon to the groups A and B with low bpp and ml bs support, and is labeled with the letter D. Isolate C143, labeled with the letter E, is a sister taxon to all *D. purpureum* isolates with high support (1:00 bpp and ≥ 99% ml bs), and could be considered a separate species. This claim is also supported by the genetic distance matrices shown in Tables 4-5. It can be noted that the genetic distance of isolate C143 sequence from other sequences of *D. purpureum* isolates is greater than the genetic distance between any of the other isolates of *D. purpureum*. In the 5.8S rDNA molecular phylogenetic tree, group C is retained with low support, group B is divided into two groups, and isolate C143 is more distant from other *D. purpureum* isolates than *D. macrocephalum,* which also supports the claim that it is a different species.

Fourth, an attempt was made to align the ITS rDNA sequences within group 4 isolates. It was noted that ITS rDNA sequences were not alignable within all group 4 dictyostelid species, or among all the isolates of *D. purpureum* isolates. However, within the different groups A, B and C, ITS rDNA sequences can be aligned. Isolates NB1B 2271, and C143 are not alignable with any of the other isolates of *D. purpureum*. These results are informative, because although we do not have a high support of bpp and ml bs for all of the three groups from Mehdiabati et al. (2009), the ITS rDNA alignment within the three groups support their presence. Additionally, the lack of alignment of the isolates NB1B 2271 and C143 with the rest of the isolates supports the claim that they belong to two new groups (D and E), or probably to a different species in the case of isolate C143.

The morphological studies of *D. purpureum* isolates indicated similar morphological characteristics as previously described in the literature. These are sori with dark or black color, aggregation toward the center in streams, slug migration after stalk formation, elliptical spores without polar granules, and positive phototropism (Olive 1991, Raper 1984, Hagiwara 1989). These characteristics confirm that the studied isolates belong to the species *D. purpureum.* Spore dimensions, as can be seen from Figures 17-19, are variable between the different isolates. However, no clear conclusion could be drawn from the results about the differences between the isolates. The study of the sori color indicated that there is a difference between the isolates M8B and MK11B 2522, with gray color that turns to black as they mature, and the rest of the isolates, with brown/purple color that becomes darker with maturity. The two isolates with black sori are sister taxa in the phylogenetic trees which include only the studied isolates of *D. purpureum* with high support (0.97 bpp and 79% ml bs) in the combined 5.8S and 18S rDNA trees, as seen in Figure 11, and fall within group B when including other isolates of *D. purpureum.* To infer

whether isolates with black sori color comprise a subgroup within *D. purpureum* isolates, it is necessary to study the sori color of the rest of the isolates of *D. purpureum* obtained from GenBank.

Geographical distance may also affect the phylogenetic relationships between *D. purpureum* isolates. In Figure 10, the two isolates from The Great Smoky Mountains are grouped together. The three isolates which originated from Costa Rica are also grouped together, as shown in Figures 9 and 11. This could be explained by spore dispersal within the same localities (Swanson et al. 2002).

Positive mating tests were determined from the formation of macrocysts, which are part of the sexual life cycle in dictyostelids (Raper 1984). Macrocyst formation was enhanced under dark conditions, and with the addition of Bonner salt solution, which provides calcium ions important in cell fusion (Nickerson and Raper 1973). Only homothallic macrocysts were observed for the two isolates Za2a OH216 and TRII-1 OH278. However, there was a clear indication that macrocysts are formed mostly within isolates of the same group, rather than between isolates that belong to different groups as reported by Mehdiabadi et al. (2009). This macrocyst formation provides additional support for the presence of the three groups A, B, and C (Mehdiabadi et al. 2009).

For future research, it would be necessary to study and sequence additional isolates of *D. purpureum* from additional distinct localities to further confirm whether the morphologically identified isolates as the species of *D. purpureum* comprise a monophyletic groud within the dictyostelids, and to better resolve the internal phylogeny of *D. purpureum*.

Conclusions

The molecular phylogenetic trees indicated that isolates of *D. purpureum* were more closely related to each other than to other species of dictyostelids. However, several subgroups were noted within isolates of *D. purpureum*. The morphological studies indicated similar morphological characteristics for *D. purpureum* isalotes, while the main variation is the color of the sorus, which varies in its intensity among the different isolates from pale purple to black. In several cases, isolates from the same localities were also more closely related to each other within the total isolates of *D. purpureum*, which suggests that geographical distance may have an effect on the phylogenetic relationship among *D. purpureum* isolates.

Literature Cited

Abe, K., H. Orii, Y. Okada, Y. Saga, and K. Yanagisawa. 1984. Anovel cyclic AMP metabolism exhibited by giant cells and its possible role in the sexual development of *Dictyostelium discoideum.* Developmental Biology 104:477-483.

Abràmoff, M. D., P. J. Magalhães, and S. J. Ram. 2004. Image processing with ImageJ. Biophotonics International 11:36-43.

Adl, S. M., A. G. B. Simpson, C. E. Lane, J. Lukes, D. Bass, S. S. Bowser, M. W. Brown, F. Burki, M. Dunthorn, V. Hampl, A. Heiss, M. Hoppenrath, E. Lara, L. Le Gal, D. H. Lynn, H. Mcmanus, E. A. D. Mitchell, S. E. Mozley-Stanridge, L. W. Parfrey, J. Pawlowski, S. Rueckert, L. Shadwick, C. L. Schoch, A. Smirnov, and F. W. Spiegel. 2012. The revised classification of eukaryotes. Journal of Eukaryotic Microbiology 59:429-493.

Annesley, S. J., and P. R. Fisher. 2009. *Dictyostelium discoideum*-a model for many reasons. Molecular and Cellular Biochemistry 329:73-91.

Blaskovics, J. C., and K. B. Raper. 1957. Encystment stages of *Dictyostelium*. The Biological Bulletin 113:58-88.

Bloomfield, G. 2013. Sex in dictyostelia. Pages 129-148 *in* Romeralo, M., S. Baldauf and R. Escalante (eds.), Dictyostelids Evolution, Genomics, and Cell Biology. Springer-Verlag Berlin Heidelberg. Berlin, Heiderberg.

Bonner, J. 2013. The evolution of the cellular slime molds. Pages 183-191 *in* Romeralo, M., S. Baldauf and R. Escalante (eds.), Dictyostelids Evolution, Genomics, and Cell Biology. Springer-Verlag Berlin Heidelberg. Berlin, Heiderberg.

Bonner, J. T., and L. J. Savage. 1947. Evidence for the formation of cell aggregates by chemotaxis in the development of the slime mold *Dictyostelium discoideum*. Journal of Experimental Zoology 106:1-26.

Budniak, A. A., and D. H. O'Day. 2012. Microcysts: The third developmental pathway of social amoebozoans. Protist 163:2-14.

Cavender, J. C., and K. B. Raper. 1965. The Acrasieae in nature. I. Isolation. American Journal of Botany 52:294-296.

Cavender, J. 2013. A global overview of dictyostelid ecology with special emphasis in North American forest. Pages 149-166 *in* Romeralo, M., S. Baldauf and R. Escalante (eds.), Dictyostelids Evolution, Genomics, and Cell Biology. Springer-Verlag Berlin Heidelberg. Berlin, Heiderberg.

Chagla, A. H., K. E. Lewis, and D. H. O'Day. 1980. Ca^{2+} and cell fusion during sexual development in liquid cultures of *Dictyostelium discoideum*. Experimental Cell Research 126:501-505.

Cotter, D. A., and K. B. Raper. 1966. Spore germination in *Dictyostelium discoideum*. Proceedings of the National Academy of Sciences of the United States of America 56:880-887.

Darriba, D., G. L. Taboada, R. Doallo, and D. Posada. 2012. jModelTest 2: More models, new heuristics and parallel computing. Nature Methods 9:772.

Erdos, G. W., A. W. Nickerson, and K. B. Raper. 1973. The fine structure of macrocyst germination in *Dictyostelium mucoroides*. Developmental Biology 32:321-330.

Filosa, M. F., and R. E. Dengler. 1972. Ultrastructure of macrocyst formation in the cellular slime mold, *Dictyostelium mucoroides*: Extensive phagocytosis of amoebae by a specialized cell. Developmental Biology 29:1-16.

Gouy, M., S. Guindon, and O. Gascuel. 2010. SeaView version 4: A multiplatform graphical user interface for sequence alignment and phylogenetic tree building. Molecular Biology and Evolution 27:221-224.

Guindon, S., and O. Gascuel. 2003. A simple, fast, and accurate algorithm to estimate large phylogenies by maximum likelihood. Systematic Biology 52:696-704.

Guindon, S., J. F. Dufayard, V. Lefort, M. Anisimova, W. Hordijk, and O. Gascuel. 2010. New algorithms and methods to estimate maximum-likelihood phylogenies: assessing the performance of PhyML 3.0. Systematic biology 59:3:307-321.

Hagiwara, H. 1989. The Taxonomic Study of Japanese Dictyostelid Cellular Slime Molds. National Science Museum, Tokyo, Japan.

Hagiwara, H. 1992. Two forms of *Dictyostelium purpureum* OLIVE in Japan. Bulletin of the National Science Museum, Series B, Botany 18:7-15.

Hagiwara, H. 2007. Preliminary study of sexual segregation in dictyostelids. Bulletin of the National Science Museum, Series B, Botany 33:1-8.

Hall, T. A. 1999. BioEdit: a user-friendly biological sequence alignment editor and analysis program for windows 95/98/NT. Nucleic Acids Symposium Series 41:95-98.

Januszewska, N. 2011. Molecular systematics of dictyostelids: a case for single genus. Published Doctoral Dissertation, Anglia Ruskin University, England.

Kearse, M., R. Moir, A. Wilson, S. Stones-Havas, M. Cheung, S. Sturrock, S. Buxton, A. Cooper, S. Markowitz, C. Duran, T. Thierer, B. Ashton, P. Mentjies, and A. Drummond. 2012. Geneious Basic: an integrated and extendable desktop software platform for the organization and analysis of sequence data. Bioinformatics 28:1647-1649.

Lewis, K. E., and D. H. O'Day. 1976. Sexual hormone in the cellular slime mould *Dictyostelium purpureum*. Canadian Journal of Microbiology 22:1269-1273.

Medlin, L., H. J. Elwood, S. Stickel, and M. L. Sogin. 1988. The characterization of enzymatically amplified eukaryotic 16S-like rRNA-coding regions. Gene 71:491-499.

Mehdiabadi, N. J., M. R. Kronforst, D. C. Queller, and J. E. Strassmann. 2009. Phylogeny, reproductive isolation and kin recognition in the social amoeba *Dictyostelium purpureum*. Evolution, 63:542-548.

Myre, M. A. 2012. Clues to c-secretase, huntingtin and Hirano body normal function using the model organism Dictyostelium discoideum. Journal of Biomedical Science 19:41.

Nickerson, A. W., and K. B. Raper. 1973. Macrocysts in the life cycle of the Dictyosteliaceae. I. Formation of the macrocysts. American Journal of Botany 60:190-197.

O'Day, D. H., and A. Keszei. 2012. Signalling and sex in the social amoebozoans. Biological Reviews 87:313-329.

Perrigo, A. L. 2013. Diversity underfoot: Systematics and biogeography of the dictyostelid social amoebae. Published Doctoral Dissertation, Uppsala University, Uppsala, Sweden.

Perrigo, A. L., S. L. Baldauf, and M. Romeralo. 2013. Diversity of dictyostelid social amoebae in high latitude habitats of Northern Sweden. Fungal Diversity 58:185-198.

Raper, K. B. 1984. The Dictyostelids. Princeton University Press, Princeton, New Jersey.

Romeralo, M., R. Escalante, and S. L. Baldauf. 2012. Evolution and diversity of dictyostelid social amoebae. Protist 163:327-343.

Romeralo, M., F. W. Spiegel, and S. L. Baldauf. 2010. A fully resolved phylogeny of the social amoebas (Dictyostelia) based on combined SSU and ITS rDNA sequences. Protist 161:539-548.

Romeralo, M., S. L. Baldauf, and J. C. Cavender. 2009. A new species of cellular slime mold from southern Portugal based on morphology, ITS and SSU sequences. Mycologia 101: 269-274.

Romeralo, M., J. C. Cavender, J. C. Landolt, S. L. Stephenson, and S. L. Baldauf. 2011. An expanded phylogeny of social amoebas (Dictyostelia) shows increasing diversity and new morphological patterns. BMC Evolutionary Biology 11:84.

Romeralo, M., R. Escalante, L. Sastre, and C. Lado. 2007. Molecular systematics of dictyostelids: 5.8S ribosomal DNA and internal transcribed spacer region analyses. Eukaryotic Cell 6:110-116.

Romeralo, M., and O. Fiz-Palacios. 2013. Evolution of dictyostelid social amoebas inferred from the use of molecular tools. Pages 149-166 *in* Romeralo, M., S. Baldauf and R. Escalante (eds.), Dictyostelids Evolution, Genomics, and Cell Biology. Springer-Verlag Berlin, Heidelberg, Berlin, Heiderberg, Germany.

Romeralo, M., O. Fiz-Palacios, C. Lado, and J. C. Cavender. 2007. A new concept for *Dictyostelium sphaerocephalum* based on morphology and phylogenetic analysis of nuclear ribosomal internal transcribed spacer region sequences. Canadian Journal of Botany 85:104-110.

Romeralo, M., S. N. Rajguru, J. D. Silberman, J. C. Landolt, O. Fiz, and S. L. Stephenson. 2010. Population structure of the social amoeba *Dictyostelium rosarium* based on rDNA. Fungal Ecology 3:379-385.

Ronquist, F., M. Teslenko, P. van der Mark, D. L. Ayres, A. Darling, S. Hohna, B. Larget, L. Liu, M. A. Suchard, J. P. Huelsenbeck. 2012. MrBayes 3.2: Efficient Bayesian phylogenetic inference and model choice across a large model space. Systematic Biology 61:539-542.

Sambrook, J., D. W. Russell. 2001. Molecular Cloning. Cold Spring Harbor Laboratory Press, Cold Spring Harbor, New York.

Schaap, P. 2007. Evolution of size and pattern in the social amoebas. BioEssays 29:635-644.

Schaap, P. 2011. Evolutionary crossroads in developmental biology: *Dictyostelium discoideum*. Development 138:387-396.

Schaap, P., T. Winckler, M. Nelson, E. Alvarez-Curto, B. Elgie, H. Hagiwara, J. Cavender, A. Milano-Curto, D. E. Rozen, T. Dingermann, R. Mutzel, and S. L. Baldauf. 2006. Molecular phylogeny and evolution of morphology in the social amoebas. Science 314:661-663.

Stephenson, S. L., and J. C. Landolt. 1992. Vertebrates as vectors of cellular slime molds in temperate forests. Mycological Research 96:670-672.

Sucgang, R., A. Kuo, X. Tian, W. Salerno, A. Parikh, C. L. Feasley, E. Dalin, H. Tu, E. Huang, K. Barry, E. Lindquist, H. Shapiro, D. Bruce, J. Schnutz, A. Salamov, P. Fey, P. Guadet, C. Anjard, M. M. Babu, S. Basu, Y. Bushmanova, H. van der Well, M. Katoh-Kurasawa, C. Dinh, P. M. Coutinho, T. Saito, M. Elias, P. Schaap, R. R. Kay, B. Henrissat, L. Eichinger, F. Rivero, N. H. Putnam, C. M. West, W. F. Loomis, R. L. Chisholm, G. Shaulsky, J. E. Strassmann, D. C. Queller, A. Kuspa, and I. V. Grigoriev. 2011. Comparative genomics of the social amoebae *Dictyostelium discoideum* and *Dictyostelium purpureum*. Genome Biology 12:R20.

Suzuki, K., and K. Yanagisawa. 1989. Environmental factors inducing sexual development in *Dictyostelium discoideum*. The Botanical Magazine, Tokyo 102:53-61.

Swanson, A., E. M. Vadell, and J. C. Cavender. 1999. Global distribution of forest soil dictyostelids. Journal of Biogeography 26:133-148.

Swanson, A. R., F. W. Spiegel, and J. C. Cavender. 2002. Taxonomy, slime molds, and the questions we ask. Mycologia 94:968-979.

Toama, M. A., and K. B. Raper. 1967. Microcysts of cellular slime mold *Polysphondylium pallidum* I. Factors influencing microcyst formation. Journal of Bacteriology 94:1143-1149.

Appendices

Appendix 1: Copyright Permissions.

Figure 1: From Adl et al. (2012).

Reproduced with permission of the publisher, John Wiley and Sons, via Copyright Clearance Center.

License date: April 18, 2015.

License number: 3611991221088.

Figure 2 and Figure 4: From O'Day and Keszei (2012).

Reproduced with permission of the publisher, John Wiley and Sons, via Copyright Clearance Center.

License date: April 18, 2015.

License number: 3612000598928.

Figure 6: From Mehdiabadi et al (2009).

Reproduced with permission of the publisher, John Wiley and Sons, via Copyright Clearance Center.

License date: April 18, 2015.

License number: 3612020130439.

Figure 21: From Schaap et al (2006).

Reproduced with permission of the publisher, The American Association for the Advancement of Science, via Copyright Clearance Center.

License date: April 18, 2015.

License number: 3612010633234.